MOLECULAR AND CELLULAR BIOLOGY, May 2008, p. 2952–2970 Vol. 28, No. 9
0270-7306/08/$08.00+0 doi:10.1128/MCB.00248-08

Protein Kinase A Represses Skeletal Myogenesis by Targeting Myocyte Enhancer Factor 2D▽†

Min Du,[1,2] Robert L. S. Perry,[1] Nathaniel B. Nowacki,[1] Joseph W. Gordon,[1] Jahan Salma,[1] Jianzhong Zhao,[1] Arif Aziz,[1] Joseph Chan,[1] K. W. Michael Siu,[1,2,3] and John C. McDermott[1,2]*

Department of Biology, York University, Toronto M3J 1P3, Ontario, Canada[1]; Centre for Research in Mass Spectrometry, York University, Toronto M3J 1P3, Ontario, Canada[2]; and Department of Chemistry, York University, Toronto M3J 1P3, Ontario, Canada[3]

Received 14 February 2008/Accepted 19 February 2008

Activation of protein kinase A (PKA) by elevation of the intracellular cyclic AMP (cAMP) level inhibits skeletal myogenesis. Previously, an indirect modulation of the myogenic regulatory factors (MRFs) was implicated as the mechanism. Because myocyte enhancer factor 2 (MEF2) proteins are key regulators of myogenesis and obligatory partners for the MRFs, here we assessed whether these proteins could be involved in PKA-mediated myogenic repression. Initially, in silico analysis revealed several consensus PKA phosphoacceptor sites on MEF2, and subsequent analysis by in vitro kinase assays indicated that PKA directly and efficiently phosphorylates MEF2D. Using mass spectrometric determination of phosphorylated residues, we document that MEF2D serine 121 and serine 190 are targeted by PKA. Transcriptional reporter gene assays to assess MEF2D function revealed that PKA potently represses the transactivation properties of MEF2D. Furthermore, engineered mutation of MEF2D PKA phosphoacceptor sites (serines 121 and 190 to alanine) rendered a PKA-resistant MEF2D protein, which efficiently rescues myogenesis from PKA-mediated repression. Concomitantly, increased intracellular cAMP-mediated PKA activation also resulted in an enhanced nuclear accumulation of histone deacetylase 4 (HDAC4) and a subsequent increase in the MEF2D-HDAC4 repressor complex. Collectively, these data identify MEF2D as a primary target of PKA signaling in myoblasts that leads to inhibition of the skeletal muscle differentiation program.

Skeletal muscle development has become a paradigm for the study of cellular differentiation (9, 10, 39, 49, 78). During ontogeny, precursor cells residing in the mesodermal segments flanking the embryonic anterior-posterior axis adjacent to the neural tube, named somites, commit to the muscle lineage as mononucleated, proliferating myoblasts (4, 8, 70). Myogenesis is initiated in response to appropriate cues, and subsequently the myoblasts migrate, withdraw from the cell cycle, and terminally differentiate to form multinucleated myotubes, forming the fundamental building blocks of the extensive postnatal architecture of vertebrate skeletal muscle (4, 8). Considerable molecular analysis has revealed the role of two key transcriptional regulatory factor families, the muscle regulatory factors (MRFs) and myocyte enhancer factors 2 (MEF2s), that regulate muscle-specific gene expression and differentiation in a complex, evolutionarily conserved manner (7, 62). The MRFs (MyoD, Myf5, myogenin, and MRF4) belong to the basic helix-loop-helix superfamily of DNA binding proteins, which bind to the E box *cis* element (CANNTG) that is found in the regulatory regions of most muscle-specific genes (54). The MEF2 family of transcription factors (MEF2A to -D) are crucial in regulating skeletal (51, 55, 78), cardiac (19, 36), and smooth muscle differentiation (3, 14, 35), neuronal survival (42) and T-cell activation (77). The amino termini of MEF2 proteins are conserved among all family members and consist of a 58-amino-acid MADS domain (67) and a 28-amino-acid MEF2 domain that collectively mediate DNA binding to a cognate *cis* element with the consensus sequence (T/C)TA(A/T)$_4$TA(G/A), dimerization, and cofactor interaction (47). The MEF2 transactivation domain is located in the carboxy terminus and is subjected to extensive alternative splicing and posttranslational modification by phosphorylation, acetylation, and sumoylation (7, 13, 25, 26, 40, 56, 76).

Extensive analysis has identified a variety of extracellular cues that regulate myogenesis in both a positive and negative fashion (4, 16). In particular, signal transduction pathways initiated by growth factors such as insulin-like growth factor 1 (IGF1), transforming growth factor beta (TGF-β), epidermal growth factor (EGF), and platelet-derived growth factor have all been shown to modulate skeletal muscle differentiation (20–22, 28, 29, 61, 71, 75). However, the intracellular pathways by which these signals are transmitted and ultimately converge on the transcriptional machinery to modulate gene expression, and thus differentiation, have been much more elusive.

Elevation of intracellular cyclic AMP (cAMP) levels upon adenylate cyclase activation is the archetypal cellular second messenger system and serves as a potent regulator of multiple cellular processes, including the regulation of gene expression. As a classical effector of the G-protein-coupled receptor, responding to increased intracellular cAMP, protein kinase A (PKA) is likewise involved in regulation of diverse biological

* Corresponding author. Mailing address: Department of Biology, York University, 4700 Keele Street, Toronto M3J 1P3, Ontario, Canada. Phone: (416) 736-2100, ext. 30389. Fax: (416) 736-5698. E-mail: jmcderm@yorku.ca.

† Supplemental material for this article may be found at http://mcb.asm.org/.

▽ Published ahead of print on 25 February 2008.

processes, including cell proliferation (41, 68, 69), muscle differentiation (11, 33, 74), and neuronal survival (27, 34, 64). Inactive PKA is a heterotetramer composed of two catalytic and two regulatory subunits. Elevation of intracellular cAMP levels promotes the dissociation of the regulatory subunits from the catalytic subunits, resulting in the active catalytic subunits phosphorylating protein substrates on serine/threonine residues. Previously, it was shown that elevated intracellular cAMP levels or engineered constitutively activated PKA potently inhibits myoblast differentiation, although the molecular mechanism of inhibition was unclear (33, 74). PKA was shown to phosphorylate the MRF family member myogenin, but the sites phosphorylated were dispensable for the inhibitory effect of PKA on myogenesis, and therefore an indirect mechanism for myogenic repression was proposed (33).

Since MEF2 is an obligatory partner for the MRFs in the myogenic program, we performed an in silico analysis of MEF2 proteins and found that each MEF2 protein contained potential PKA phosphoacceptor sites, defined by the consensus sequence $(R/K)_2X(S/T)$ or $(R/K)X(S/T)$ (phosphoacceptor residues are shown in italics). Thus, we questioned whether MEF2 might be a primary target of PKA-mediated myogenic repression. Indeed, MEF2s have already been shown to be sensitive to several signal transduction cascades, and their posttranslational regulation by PKC (56), p38 mitogen-activated protein kinase (MAPK) (26, 56), extracellular signal-regulated kinase 5 (ERK5) (31, 76), CDK5 (23), and CK2 (48) has been well documented. In addition, a further level of posttranslational control of the MEF2s involves protein-protein interactions. MEF2 has previously been shown to physically interact with class II histone deacetylases (HDACs) (including HDAC4, -5, -7, and -9) (32, 38, 45), GATA4 (50), MyoD (46), p300 (65), Sp1 (24, 59), Smad2 (63), myocardin (15), and MASTR (15). Thus, combinations of posttranslational modifications and interactions with regulatory protein partners create a unique code for the complex regulation of MEF2 function, underlying the diverse roles that MEF2 presides over in development and postnatal physiology.

In this report, we document that PKA directly targets MEF2D and represses its transactivation properties in differentiating muscle cells. Using in vitro and in vivo strategies, two novel PKA phosphoacceptor sites on MEF2D have been identified by mass spectrometry (MS). Reconstitution of MEF2 function by overexpression of a MEF2D protein with neutralizing mutations of the PKA phosphoacceptor sites efficiently restores myogenesis by rendering the cells resistant to the inhibitory effect of PKA or elevated cAMP levels. In addition to the direct phosphorylation and repression of MEF2 transactivation properties, increased intracellular cAMP levels in myoblasts caused endogenous HDAC4 to translocate into the nucleus, increasing the stoichiometry of the association of HDAC4 with MEF2D. Therefore, direct targeting and repression of MEF2D transactivation properties in combination with an increased nuclear association between MEF2D and the HDAC4 corepressor are proposed as the primary mechanism leading to PKA-mediated myogenic repression.

MATERIALS AND METHODS

Plasmids. The muscle creatine kinase promoter-enhanced green fluorescent protein (MCK-EGFP) construct was a kind gift from A. Ferrer-Matinez (Universitat de Barcelona, Spain). The expression vector for the catalytic subunit of PKA (pFC-PKA) was a kind gift from Zixu Mao (Brown University). Full-length MEF2D was isolated by reverse transcription-PCR from C2C12 myoblasts and cloned into the pcDNA3 vector (Invitrogen) as pcDNA3-MEF2D or into a modified pcDNA4/TO/TAP vector (13) to construct pcDNA4/TO/TAP-MEF2D. Gal4-MEF2D (87-507) and glutathione *S*-transferase (GST)-MEF2D were described in previous publications (12, 76). Reporter gene constructs pMCK-Luc and Gal4-Luc (56) were previously described (18, 56). pGL3-4 × MEF2-Luc was made from pGL3-MEF2-Luc (63), with three additional copies of the MEF2 site inserted.

Cell culture and transfections. Cells were maintained in growth medium (GM) containing Dulbecco's modified Eagle's medium (DMEM; Gibco), penicillin, and streptomycin with 10% fetal bovine serum (HyClone) at 5% CO_2. Transient transfections were performed using the standard calcium phosphate precipitation method (30). Cells were washed with phosphate-buffered saline (PBS) and harvested 48 h after transfection. C2C12 myoblast differentiation was induced by culture in differentiation medium (DM) containing DMEM, penicillin, and streptomycin with 5% horse serum (HyClone) at 5% CO_2 for 48, 72, or 96 h.

In vitro kinase assay. The GST pull-down assay was described in a previous publication (76). Briefly, 2.5 μg of purified recombinant GST-MEF2D was incubated with either the heat-inactivated or the active purified catalytic subunit of PKA (Biolab) and with [γ-^{32}P]ATP or unlabeled ATP (for MS analysis) for 30 min and denatured by heating for 4 min at 95°C in sodium dodecyl sulfate (SDS) sample buffer (Sigma). Protein samples were separated by 10% SDS-polyacrylamide gel electrophoresis (SDS-PAGE) and then either exposed to X-ray film (Kodak X-Omat) for 16 h to detect ^{32}P incorporation or stained with Coomassie blue to visualize proteins for MS analysis.

TAP. Cos7 cells (8×10^6) were transiently transfected with pcDNA4/TO/TAP-MEF2D, with or without pFC-PKA. The purification scheme and tandem affinity purification (TAP) vector system was described previously (12). Cells were lysed by three quick-freeze–thaw cycles in IPP150 lysis buffer with protease inhibitors. The cell lysate was incubated with rabbit immunoglobulin G (IgG) resin (Sigma) overnight on a rotator. After washing of the resin three times with IPP150 buffer, AcTEV protease (Invitrogen) was incubated with TAP-MEF2D for 2 h at 16°C to cleave off CBP-MEF2D. Proteins were then incubated with calmodulin resin (Stratagene) in IPP150 calmodulin binding buffer for 1 h at 4°C. After three washes with IPP150 calmodulin binding buffer, CBP-MEF2D was eluted with SDS sample buffer, heated for 4 min at 95°C, and then separated by 10% SDS-PAGE. Coomassie blue staining was used to visualize the proteins.

In-gel trypsin digestion. Coomassie blue-stained protein bands were excised, cut into small pieces, washed with 50% acetonitrile–25 mM ammonium bicarbonate, and placed on a shaker for 15 min (three times). Gel pieces were reduced by incubation with 10 mM dithiothreitol in 50 mM ammonium bicarbonate (freshly made) for 30 min at 50°C and then washed twice with acetonitrile, followed by incubation with 55 mM iodoacetamide (Sigma) in 50 mM ammonium bicarbonate (freshly made) for 20 min in the dark at room temperature (RT). The gel pieces were then washed twice with acetonitrile, air dried, rehydrated with 12.5 ng/μl trypsin (sequencing grade; Roche) in 50 mM ammonium bicarbonate at 4°C for 1 hour, and then incubated at 37°C overnight. After overnight incubation, peptides were further extracted using 3% formic acid at 70°C for 2 min, followed by 15 min of shaking. The samples were then concentrated by centrifugation at 12,000 × *g* for 1 min.

MALDI or nano-LC MS. For matrix-assisted laser desorption ionization (MALDI) sample preparation, C_{18} μZipTips (Millipore) were used to desalt and concentrate tryptic peptides from the tryptic digests per the manufacturer's protocol. The sorbed peptides were then eluted from the ZipTips and spotted onto a MALDI target plate, using 1 μl of matrix solution (10 mg/ml α-cyano-4-hydroxycinnamic acid in 65% acetonitrile and 0.3% trifluoroacetic acid). For nano-liquid chromatography (nano-LC), a detailed strategy has been described previously (58). A Tempo nano multidimensional LC system (Eksigent Technologies, LLC, Dublin, CA) was used. Capillary reverse-phase LC-MS/MS was performed by loading 5 μl of sample digest via an autosampler onto a PepMap C_{18} 75-μm-internal-diameter by 15-cm capillary column packed with 3-μm beads with 100-Å pores. Separation was effected at a flow rate of 300 nl/min via a linear gradient of 5 to 80% acetonitrile in 0.1% formic acid over 40 min.

Peptide mapping and collision-induced dissociation (CID) were performed on a hybrid quadrupole–time-of-flight (TOF) tandem mass spectrometer (Sciex Qstar XL; Applied Biosystems/MDS), using the positive-ion reflector mode. For nano-LC-MS/MS, the reverse-phase column was coupled directly to a nanospray tip for online analysis. The hybrid quadrupole TOF instrument was optimized and calibrated daily. CID resulted in MS/MS spectra from which sequencing and identification of phosphorylation sites were possible by searching against a non-

redundant protein database (NCBI), using the search program MASCOT (Matrix Science).

Site-directed mutagenesis. The full-length pcDNA3-MEF2D construct and GAL4-MEF2D (87-507) with mutations to alanine (A) at serine 121 and serine 190 were generated using a QuikChange kit (Stratagene) according to the manufacturer's instructions. All mutations were confirmed by semiautomated DNA sequencing.

Western blot assay. Cells (1.6×10^6) were placed on ice, washed three times with ice-cold PBS, and then lysed in NP-40 lysis buffer (0.5% NP-40, 150 mM NaCl, 2 mM EDTA, 50 mM Tris-HCl [pH 8.0], 100 mM NaF, and 10 mM $Na_4P_2O_7$) with protease inhibitors (leupeptin, aprotinin, pepstatin A, and phenylmethylsulfonyl fluoride). The protein concentration was measured by the Bradford assay. Equivalent amounts of total protein (typically 10 to 25 μg) were resolved by 10% SDS-PAGE and then transferred to an Immobilon-P membrane (Millipore, Inc.), blocked with 5% milk in PBS for 1 hour at RT, and probed with anti-MEF2D (BD transduction) at 1:1,000, anti-Flag (Sigma) at 1:1,000, anti-HDAC4 (Sigma) at 1:1,000, and anti-actin (Santa Cruz) at 1:500 with 5% milk in PBS overnight at 4°C. Blots were washed three times with PBS for 10 min at RT, incubated with the appropriate secondary horseradish peroxidase-conjugated antibody (Bio-Rad) at 1:2,000 with 5% milk in PBS for 1 h at RT, and then washed three times with PBS for 10 min at RT. Chemiluminescence was used for detection per the manufacturer's instructions (Amersham Biosciences).

Limited proteolytic digestion of MEF2D. In vitro kinase assays of GST-MEF2D (full length [amino acids {aa} 1 to 507] or lacking the MADS/MEF2 domain [aa 87 to 507]) were performed as described above. Following the kinase assay, equal aliquots were taken from each protein sample to perform limited proteolysis by trypsin (sequencing grade; Roche) in a buffer containing 100 mM ammonium bicarbonate at 16°C for different time intervals. The protein/trypsin ratio was 100 to 1. Proteolysis was terminated by adding SDS sample buffer (Sigma) and heating for 4 min, followed by separation using 10% SDS-PAGE.

Transcriptional response assays. Transient transfection was performed using standard calcium phosphate precipitation methods. pCMV-β-galactosidase or pSV40-β-galactosidase was transfected as an internal control for transfection efficiency. Reporter gene constructs used were pMCK-Luc, pGL3-4 × MEF2-Luc, and Gal4-Luc. Cells were washed with PBS and cultured with GM 14 to 16 h following transfection and then harvested at 48 h posttransfection or 48 h after differentiation in DM. One hundred microliters of lysate was used to assay β-galactosidase (β-Gal) activity as an internal transfection efficiency control. Luciferase reporter assays were carried out according to the manufacturer's instructions (Promega), using a Berthold 9501 luminometer.

Nuclear-cytoplasmic extraction protocol. C2C12 cells (1.6×10^6) were placed on ice and washed three times with ice-cold PBS. Whole-cell extracts were obtained in NP-40 lysis buffer containing protease inhibitors as described above. Nuclear and cytoplasmic extracts were obtained by using NE-PER nuclear and cytoplasmic extraction reagents (Pierce Biotechnology) according to the manufacturer's instructions.

Immunocytochemistry. C2C12 cells were fixed in 4% paraformaldehyde in PBS for 10 min at RT and permeabilized with 0.3% Triton X-100 (Sigma-Aldrich Canada) for 5 min. Fixed cells were blocked with 10% goat serum in PBS for 30 min and incubated with anti-HDAC4 (1:100 in 1.5% goat serum; Sigma) overnight at 4°C. The cells were washed extensively with PBS and then incubated with anti-rabbit IgG–tetramethyl rhodamine isocyanate conjugate (1:50 in 1.5% goat serum; Sigma) for 2 h at RT. The cells were washed with PBS and mounted with Dako mounting medium (Dako). The images were captured using a Fluoview 300 microscope (Olympus).

Coimmunoprecipitation assays. Cells (5×10^6) were lysed in NP-40 lysis buffer containing protease inhibitors as described above. Five hundred micrograms of total protein was incubated with 1 μg antibody and 25 μl protein G-conjugated Sepharose beads (Santa Cruz) and placed on a rotator overnight at 4°C. The beads were then washed three times with NETN washing buffer (0.1% NP-40, 150 mM NaCl, 1 mM EDTA, and 50 mM Tris-HCl [pH 8.0]). Protein complexes were released from the beads by being heated at 95°C for 4 min in SDS sample buffer and then were separated by 10% SDS-PAGE and blotted as described above.

EMSA. DNA binding assays and extract preparation were carried out as previously described (57). Briefly, the incubation reaction mixture comprised equivalent amounts of protein (1 to 3 μg total protein), 0.2 ng of double-stranded probe, and 0.45 μg of poly(dI-dC) in a total volume of 20 μl. The electrophoretic mobility shift assay (EMSA) binding reaction buffer consisted of 10 mM HEPES (pH 7.6), 3 mM $MgCl_2$, 20 mM KCl, 1 mM dithiothreitol, and 5% glycerol. After the addition of the ^{32}P-labeled binding site probe, the reaction mixture was incubated at RT for 20 min. The reaction mixture was resolved using electrophoresis on a 4.5% nondenaturing polyacrylamide gel to separate the bound from the free fraction. The core MEF2 nucleotide sequence used in the EMSA was MEF2 (5′-CGCTCTAAAAATAACCCT-3′; the MEF2 consensus DNA binding site is underlined). Following electrophoresis, the gels were dried, and DNA-protein complexes were visualized by autoradiography after overnight exposure to X-ray film at −80°C.

MEF2 activity in cultured primary somite cells from MEF2-LacZ sensor mice treated with FSK. Primary somite cells were cultured from MEF2 sensor mouse embryos at the 20- to 25-somite stage, at 9.5 days postcoitum (dpc), as described previously (72). Briefly, embryonic tissue was dissociated by gentle pipetting in Ca^{2+}- and Mg^{2+}-free PBS to obtain a single-cell suspension. Cells were collected by centrifugation and inoculated at an initial density of 3×10^5 cells/ml in DMEM supplemented with 10% FBS. After being treated with forskolin (FSK) at final concentrations of 10 and 30 μM for 24 h, the cells were fixed in 2% paraformaldehyde-0.2% glutaraldehyde in PBS on ice for 10 min, followed by two washes in PBS for 10 min each at RT. The cells were subsequently incubated in X-Gal (5-bromo-4-chloro-3-indolyl-β-D-galactopyranoside) staining solution (5 mM ferrocyanide, 5 mM ferricyanide, 2 mM $MgCl_2$, and 1 mg/ml X-Gal) for 24 h at 37°C.

MEF2 activity in skeletal muscles treated with FSK or IBMX in the MEF2-LacZ sensor mouse. MEF2-LacZ transgenic sensor mice at 8 to 12 weeks of age were used for these studies (52). The lateral lobe of the gastrocnemius muscle of the left hind limb was injected with 100 μl FSK in PBS at a concentration of 100 μM or with 3-isobutyl-1-methylxanthine (IBMX) at a concentration of 1.5 mM. In one of the experiments, prior to the IBMX treatment, a direct intramuscular injection of barium chloride ($BaCl_2$; 1.2%) was used to cause a marked degeneration of the muscle followed by a robust regeneration which involves MEF2 activation, as we have previously described (1). The corresponding gastrocnemius muscle of the right hind limb was injected with saline and served as the control. Twenty-four hours after injection, animals were sacrificed by sodium pentobarbital injection, and 10-μm transverse sections of the gastrocnemii were mounted on gelatin-coated slides. The slides were fixed in 4% paraformaldehyde in PBS. After being washed three times with PBS, the slides were incubated with X-Gal solution at 37°C to visualize β-Gal-positive cells (5 mM ferrocyanide, 5 mM ferricyanide, 2 mM $MgCl_2$, and 1 mg/ml X-Gal in dimethylformamide), and the samples were examined using bright-field microscopy.

RESULTS

Activated PKA inhibits C2C12 muscle cell differentiation. Initially, we tested whether expression of constitutively activated PKA inhibits C2C12 myoblast differentiation, as reported by others (11, 33, 74). To further document this phenotypic observation, we studied the activation of the MCK promoter because its activation is a useful index of muscle-specific gene expression, since the promoter is highly dependent on MEF2 and E-box *cis* elements for its activation in myogenic cells (2). We used the MCK promoter fused to the GFP reporter gene as an indicator for muscle differentiation since this has the added feature of indicating the phenotype of the transfected cells as well as the activation of muscle-specific gene expression. In addition, dsRed was used as a marker of transfection efficiency. Phase-contrast and fluorescence images were taken 48 and 72 h after differentiation was initiated by serum withdrawal. PKA inhibition of C2C12 myoblast differentiation was indicated by reduced numbers of GFP-positive myotubes (Fig. 1A). Quantitative reporter gene analysis was correspondingly carried out using the MCK promoter driving the luciferase gene (Fig. 1B). These data further documented that PKA inhibited MCK promoter activity. Since the MCK promoter is highly dependent on MRF and MEF2 activity, we subsequently tested whether PKA can inhibit a MEF2-dependent reporter gene (MEF2-Luc). Exogenous expression of pFC-PKA potently suppressed wild-type MEF2D's transactivation potential in a dose-dependent manner, without nonspecific repression of the MEF2-independent pGL3-Luc backbone vector (Fig. 1C). It was also observed that overexpression

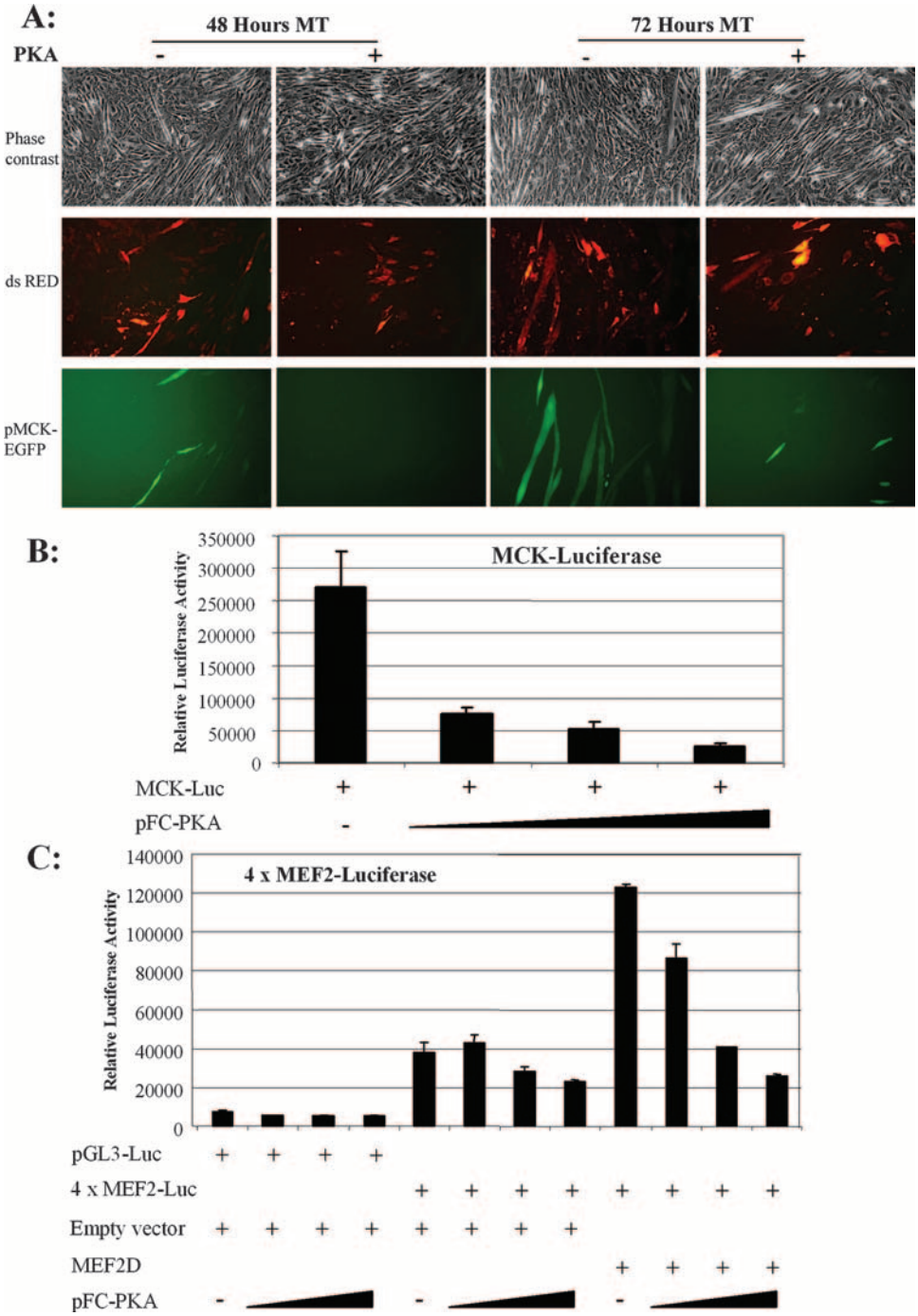

FIG. 1. PKA inhibits myogenic differentiation. (A) C2C12 myoblasts were transiently transfected with pMCK-EGFP and pCMV-dsRed2, with or without the pFC-PKA (catalytic subunit of PKA) vector, recovered in GM for 24 h, and then induced to differentiate by using 5% horse serum (DM). After 48 or 72 h in DM, phase-contrast and fluorescence images (green, pMCK-EGFP; and red, pCMV-dsRed2) were obtained. MT, myotubes. (B) C2C12 cells were transiently transfected with pMCK-Luc and increasing amounts of pFC-PKA (100 to 500 ng) and harvested 48 h after being induced to differentiate in DM. Overexpression of PKA significantly suppressed MCK-Luc in a dose-dependent manner. Data are means ± SEM (n = 3). (C) C3H10T1/2 cells were cotransfected with empty vector or pcDNA3-MEF2D and increasing amounts of pFC-PKA (0.02 to 0.2 μg) and harvested 48 h after transfection. pGL3-4 × MEF2-Luc (four copies of MEF2 binding sites driven by the luciferase reporter gene) was used as the reporter gene.

of pFC-PKA repressed MEF2-Luc activity when no MEF2D was transfected due to suppression of endogenous MEF2D in these cells. Taken together, these data identified MEF2D as a putative downstream target of PKA signaling.

PKA directly phosphorylates MEF2D in vitro. The observation that PKA represses MEF2 activity in vivo prompted us to determine whether this effect was mediated by direct phosphorylation of MEF2D by PKA by using purified components in an

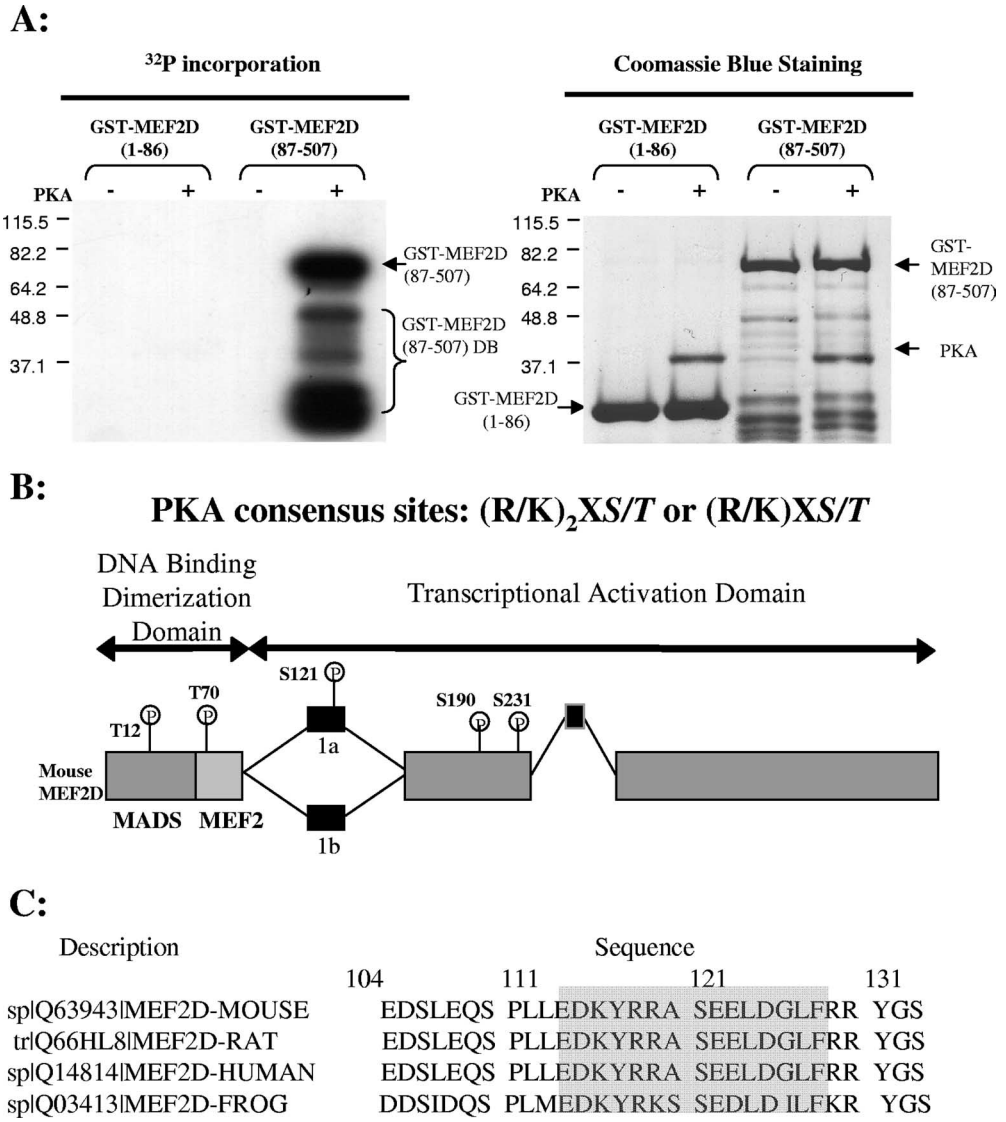

FIG. 2. PKA phosphorylates MEF2D directly in vitro. (A) Purified GST-MEF2D (MADS-MEF2 domain [aa 1 to 86 or 87 to 507]) was incubated in vitro, with or without purified PKA, with [γ-^{32}P]ATP, resolved using SDS-PAGE, visualized by Coomassie blue staining, dried, and exposed to X-ray film for 16 h after the PKA kinase assay. (B) Several cognate PKA phosphoacceptor sites were identified on mouse MEF2D by the consensus sequence $(R/K)_2X(S/T)$ or (R/K)X(S/T). (C) Ser 121 is highly conserved between MEF2D proteins from the mouse, human, rat, and frog. Residue coordinates are labeled according to mouse MEF2D.

in vitro kinase assay. Incubation of MEF2D with active PKA resulted in phosphorylation of GST-MEF2D 87-507, whereas the MADS-MEF2 amino-terminal region of MEF2D (GST-MEF2D 1-86) was not phosphorylated by PKA (Fig. 2A; see Fig. S1, S2, and S3 in the supplemental material). The lack of GST-MEF2D 1-86 phosphorylation by PKA failed to confirm the results of Wang et al., who reported PKA-mediated phosphorylation of T20 (73). In these assays, we also tested MEF2A and -C and found them to be poor substrates for PKA, and we thus concluded that these are unlikely targets of PKA (data not shown). These observations led us to the hypothesis that the unique PKA phosphoacceptor sites in MEF2D might be critical for the PKA effect on MEF2 function.

PKA typically phosphorylates proteins at the consensus site, $(R/K)_2X(S/T)$ or (R/K)X(S/T). Theoretical mapping of the PKA consensus sites on MEF2D resulted in identification of multiple putative PKA sites in MEF2D (Fig. 2B). Interestingly, Ser 121 of MEF2D is present only in the alternatively spliced exon (isoform 1a), which is expressed in C2C12 myoblasts, PC12 cells, and kidney, stomach, heart, and brain tissue (44). Evolutionary conservation of Ser 121 is indicated by comparison of MEF2D protein sequences between different species (Fig. 2C). This hypothesis thus required detailed mapping of the PKA phosphoacceptor sites on MEF2D.

Identification of novel PKA phosphorylation sites on MEF2D. Having determined that MEF2D is a direct target for PKA, we next sought to characterize the PKA phosphoacceptor sites in the MEF2D protein. In vitro kinase assays were performed, as described above, and combined with MS determination of phosphoacceptor sites. A slight shift in the mobility of the

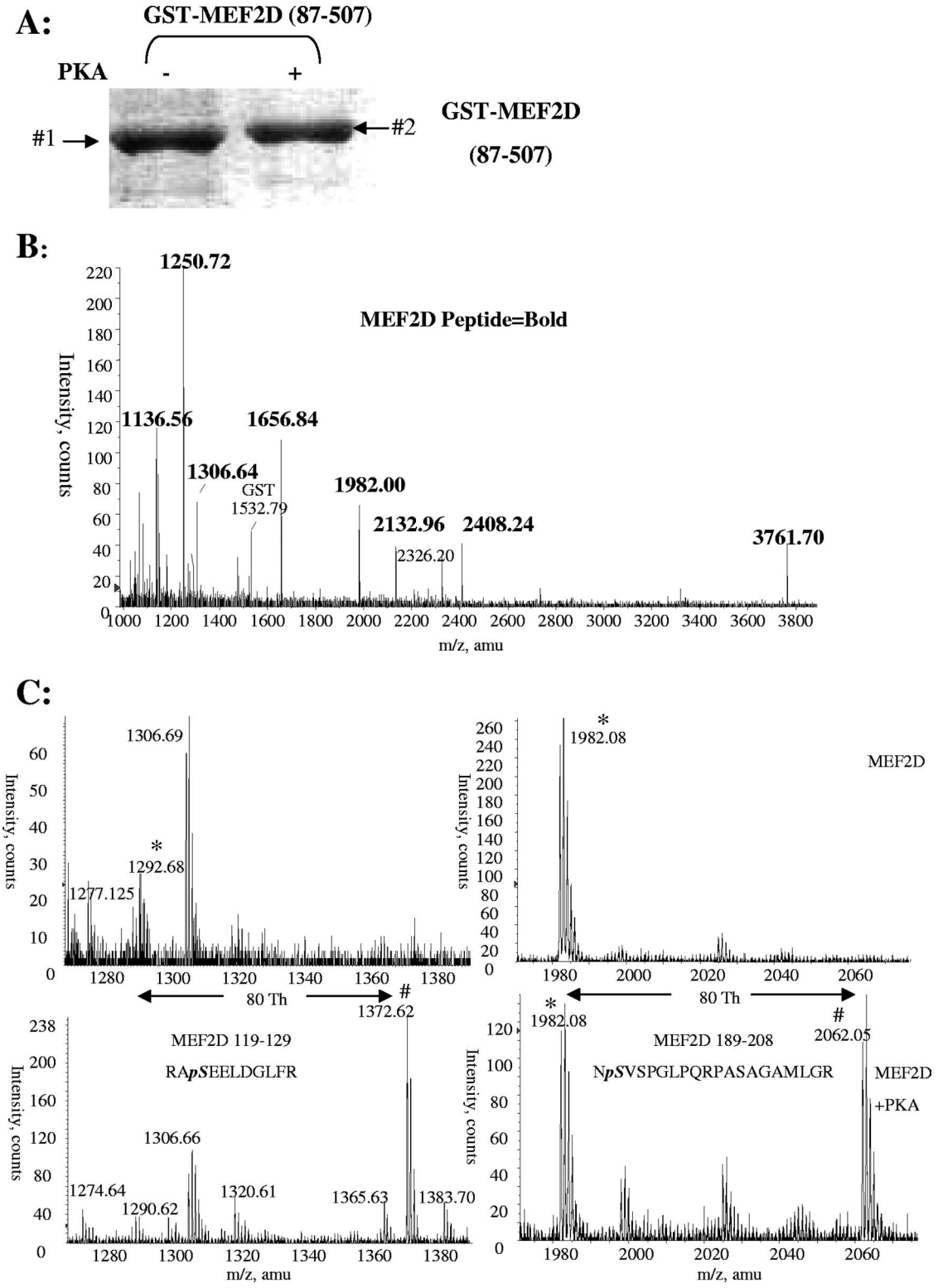

FIG. 3. Identification of PKA phosphoacceptor sites on a recombinant bacterial MEF2D protein by MS. (A) Purified GST-MEF2D (87-507) (2.5 μg) was incubated with heat-inactivated or active purified PKA for 30 min. Proteins were separated by 10% SDS-PAGE. PKA caused a slight mobility shift of MEF2D, as detected by Coomassie blue staining. (B) Tryptic peptide mapping of both bands identified them as rat MEF2D (only one spectrum is shown) by MALDI-MS. Peptide peaks assigned to MEF2D are shown in bold. (C) Mass spectral windows reveal the presence of putative phosphopeptides (#) and their nonphosphorylated analogues (*). The sequence of each phosphopeptide was identified, as shown in text above the spectra, based on subsequent MS/MS.

MEF2D protein band by PKA phosphorylation was evident (Fig. 3A, band #2). Both MEF2D protein bands were excised and digested in-gel with trypsin. The samples were subjected to MALDI-MS and MS/MS analyses. Both protein bands were identified as MEF2D by tryptic peptide mapping analysis of the MALDI-TOF MS spectral results (only one spectrum is shown in Fig. 3B). The peaks identified to have originated from MEF2D tryptic peptides were labeled in bold; these were among the most intense peaks in the spectrum. The spectrum also contained a peptide of GST.

Pairwise comparisons of the tryptic peptide fingerprints from PKA-treated and untreated (control) samples revealed the presence of two putative phosphopeptides. Figure 3C shows mass spectral windows for PKA-negative (upper panels) and -positive (lower panels) samples. Protonated phosphopeptides MEF2D 119-129 phospho-(RASEELDGLFR), with an *m*/*z* value of 1,372.66 Thomson units (Th; corresponds to Da/e), and 189-208 phospho-(NSVSPGLPQRPASAGAMLGR), with an *m*/*z* value of 2,062.06 Th, were evident only in the PKA-treated sample. In contrast, the untreated sample showed only the nonphosphorylated analogues, at *m*/*z* values that are 80 Th lower, i.e., 1,292.68 and 1,982.08 Th, respectively (phosphorylation adds 79.97 Da to the mass of a serine or threonine residue).

To confirm and pinpoint the phosphorylation sites on the two putative phosphopeptides, MS/MS was performed. The CID spectra of the 1,372.66- and 2,062.06-Th ions are shown in Fig. 4A and B, respectively. Figure 4A shows clear serial *y* and *b* fragment ions that led to the identification of the peptide as RApSEELDGLFR. The loss of 98 Th, H_3PO_4, was evident from two fragment ions, the internal fragment ion pSEE (426.21 Th) and the y_{10} ion (1,216.66 Th), to give their nonphosphorylated analogues, at 328.13 Th and 1,118.59 Th, respectively. These observations plus the fact that this peptide contains only one serine and no threonine residue allowed us to place the phosphorylation site at Ser 121, whose placement also fits the consensus PKA motif [$(R/K)_2X(S/T)$]. Fig. 4B shows the MS/MS results for the second putative phosphorylated peptide. The presence of the fragment ion at 1,964.00 Th (-98 Th) confirms that the peptide is indeed phosphorylated. The MASCOT search identified that most fragment ions in the spectrum are internal ions. The relatively uninformative MS/MS spectrum was probably a consequence of the presence of two basic arginine residues, which sequestered the ionizing proton and inhibited backbone fragmentations. Fortunately, an examination of the peptide's sequence identifies only one serine residue, Ser 190 (out of a total of three), that fits the consensus motif [(R/K)X(S/T)].

To further confirm that Ser 190 is a PKA phosphoacceptor site, nano-LC-MS/MS was performed for the in-gel-digested sample. Figure 4C shows the CID spectrum of triple protonated phospho-(NSVSPGLPQRPASAGAMLGR), with an *m*/*z* value of 688.02 Th. A clear series of *y* and *b* singly or doubly protonated fragment ions was generated with this spectrum. The loss of 98 Th, H_3PO_4, was evident from three fragment ions, the b_2 ion (282.08 Th), the b_4 ion (468.12 Th), and the b_7 ion (637.34 Th), to give their nonphosphorylated analogues, at 184.06 Th, 370.16 Th, and 637.34 Th, respectively. Taken together, we can confidently identify this peptide as NpSVSPGLPQRPASAGAMLGR.

MEF2D Ser 121 and 190 phosphorylation by PKA in vivo. To investigate whether MEF2D can also be targeted by PKA in vivo, TAP methods were used to purify TAP-MEF2D from cultured cells. Cos7 cells were transiently transfected with pcDNA4/TO/TAP-MEF2D, with or without pFC-PKA. After the full TAP scheme, proteins were separated by 10% SDS-PAGE (Fig. 5A). Both bands were digested in-gel with trypsin, and the resulting peptides were analyzed by MALDI-MS and MS/MS. Both protein bands were identified as MEF2D (Fig. 5B). The mass spectra were almost identical, except for the presence of two phosphopeptides, MEF2D 119-129 (RAp SEELDGLFR), with an *m*/*z* value of 1,372.63 Th, and MEF2D 189-229 (NpSVSPGLPQRPASAGAMLGGDLNSANGACPS PVGNGYVSAR), with an *m*/*z* value of 4,050.15 Th (data for the second peptide are not shown), only in the sample where pFC-PKA was also transfected (Fig. 5C). These observations were consistent with those made in the in vitro studies described earlier. Furthermore, CID of the ion at 1,372.63 Th generated an MS/MS spectrum (Fig. 5D) that was almost identical to the one shown in Fig. 4A. CID of the 1,374.72 Th ion observed in the sample without pFC-PKA transfection identified it as a protonated peptide of human keratin, a common contaminant as a result of sample handling (data not shown). Figure 5E summarizes the above findings in the form of a schematic map containing the two novel PKA phosphoacceptor sites.

Site-directed mutagenesis of PKA phosphoacceptor sites on MEF2D and functional analysis. In order to begin to ascertain the biological role of the PKA phosphorylation sites in MEF2D regulation, neutralizing loss-of-function mutations (S to A) were constructed at the PKA phosphoacceptor sites (MEF2D S121A, MEF2D S190A, and MEF2D S121/190A).

Initially, to test whether Ser121 and Ser 190 are the only PKA phosphoacceptor sites on MEF2D, we carried out in vitro kinase assays to compare S121/190A mutant and wild-type GST-MEF2D. Consistent with the results shown in Fig. 2A, we observed no phosphorylation of GST-MEF2D (1-86) and a very robust phosphorylation of GST-MEF2D (87-507) (Fig. 6A). Conversely, we observed very weak residual phosphate incorporation with the MEF2D S121/190A mutant (Fig. 6A). Although there was some signal for GST-MEF2D S121/190A, we did not interpret this to indicate an additional bona fide PKA phosphoacceptor site since we would expect much greater phosphate incorporation in this case. It is more likely that this could be due to permissive low-level phosphorylation of a nonphysiologic phosphoacceptor site at high concentrations of kinase and substrate in the in vitro reaction mix. These data are consistent with our detailed MS data, which do not show any evidence of any other PKA phosphoacceptor sites besides MEF2D Ser 121 and 190.

Next, to address whether PKA phosphorylation of the MEF2D protein is involved in modulation of MEF2D transactivation properties, transcriptional reporter gene assays were carried out. Since the cell lines we worked with (C2C12, Cos7, and C3H10T1/2) all have substantial amounts of endogenous MEF2D expression, which complicated the analysis of mutated proteins, we used a Gal4-based system with a GAL4-luciferase reporter and GAL4 DBD-MEF2D (87-507) in these assays. The transcriptional activity of wild-type GAL4-MEF2D (87-507) was repressed by expressing pFC-PKA (Fig. 6B). How-

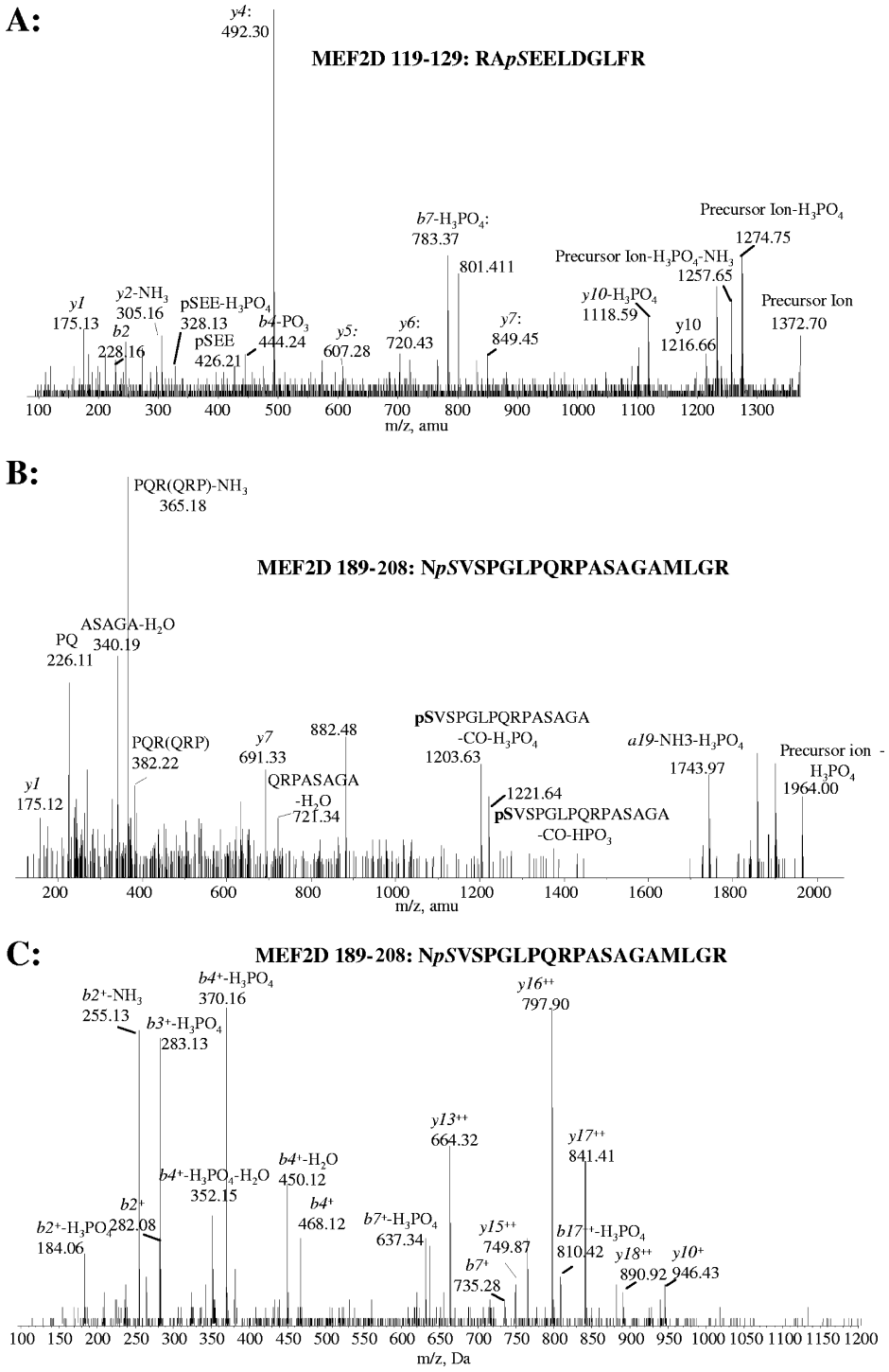

FIG. 4. Confirmation of MEF2D-PKA phosphoacceptor sites by MS/MS. The phosphopeptides were identified by CID using precursor ion scanning. (A) MEF2D 119-129 sequence (RApSEELDGLFR) (MALDI-MS/MS). (B) MEF2D 189-208 sequence (NpSVSPGLPQRPASAGAMLGR) (MALDI-MS/MS). (C) MEF2D 189-208 sequence (NpSVSPGLPQRPASAGAMLGR) (nano-LC-MS/MS). See the text for details.

ever, when GAL4-MEF2D S121/190A was cotransfected with PKA, the mutated protein was less responsive to PKA repression than wild-type GAL4-MEF2D was (Fig. 6C), thus indicating that Ser 121 and 190 are the predominant PKA phosphoacceptor sites regulating MEF2D function.

Having mapped the PKA phosphoacceptor sites on MEF2D, we next addressed the question of whether MEF2D targeting is a primary event in the PKA-mediated repression of myogenic differentiation. To test this idea, we reasoned that overexpression of the non-PKA-responsive MEF2D mutations would al-

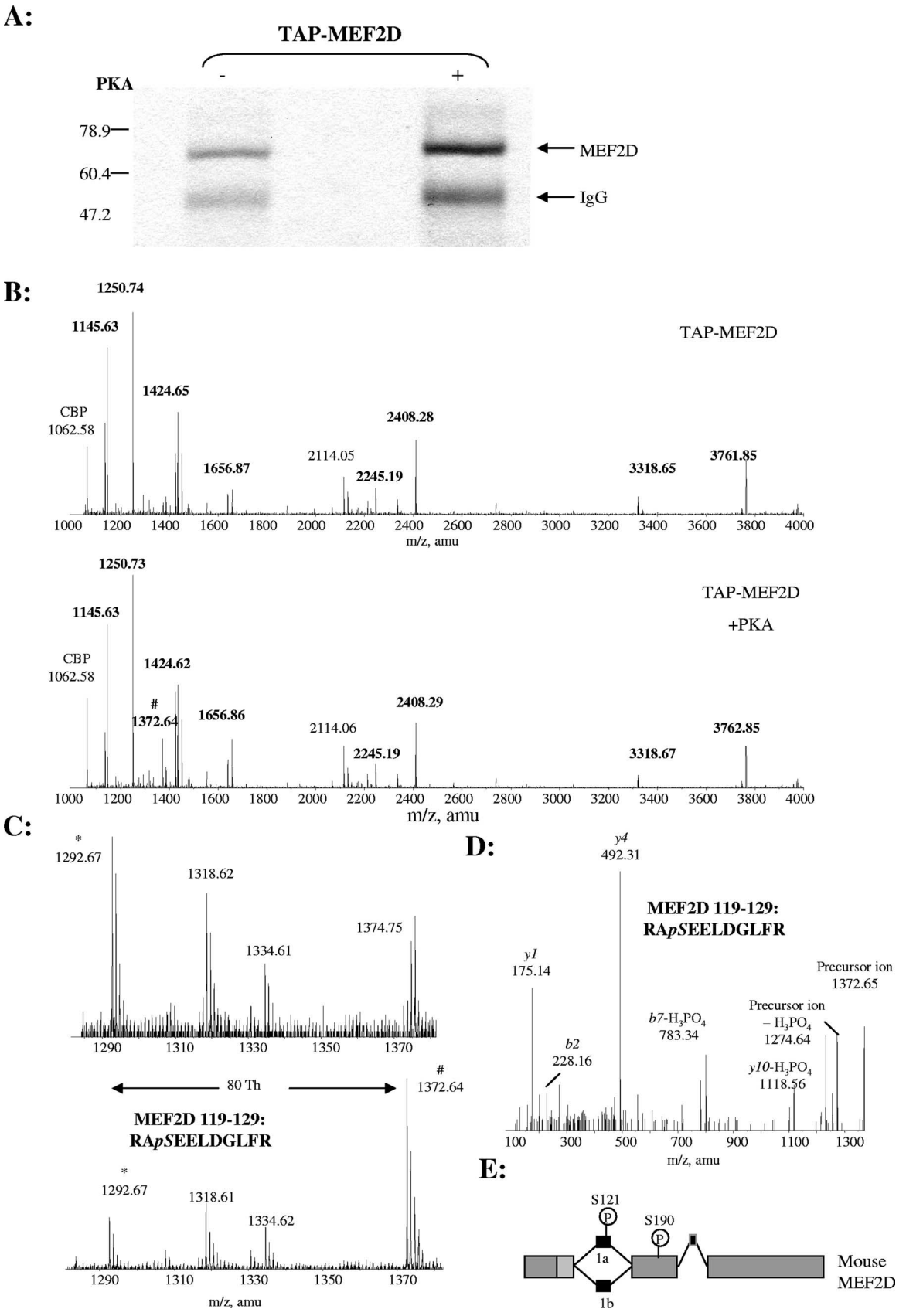

FIG. 5. Mapping of PKA phosphoacceptor sites on MEF2D in mammalian cells. (A) TAP-tagged mouse MEF2D was coexpressed with pFC-PKA in Cos7 cells. TAP-MEF2D was purified by the TAP scheme (12). Purified protein samples were separated by 10% SDS-PAGE and

low differentiation to proceed in the presence of active PKA if MEF2D repression is indeed the primary mechanism by which PKA represses myogenesis. The results of these experiments strikingly showed that MEF2D S121/190A can efficiently promote pMCK-EGFP expression and myotube formation, thus rescuing the cells from PKA-mediated repression (Fig. 7A). The number of EGFP-positive cells in each field of view was counted under each condition 48 and 96 h after differentiation to give a clear quantitative evaluation. Values are means ± standard errors of the means (SEM) calculated for eight fields of view in three individual experiments (Fig. 7B). Although forced expression of wild-type MEF2D could partially rescue differentiation in the presence of PKA, the S121/190A mutant proved significantly better at doing so. Therefore, these data demonstrate that C2C12 myoblast differentiation was potently increased and much more resistant to PKA inhibition when the cells were expressing MEF2D S121/190A.

To further confirm that the functional effects on transcriptional activation properties were due to posttranslational mechanisms and not to altered expression levels of mutated MEF2D, we assessed the levels by Western immunoblotting. Empty vector pcDNA3, full-length wild-type pcDNA3-MEF2D, MEF2D S121A, MEF2D S190A, and MEF2D S121/190A were transfected into C3H10T1/2 cells in the presence or absence of pFC-PKA. Immunoblots showed that all full-length MEF2D mutants were expressed at similar levels (Fig. 8A). Furthermore, each MEF2D vector generated a similar pattern of degradation bands [labeled DB(1-4)], a pattern we have also observed for endogenous MEF2D (Fig. 8B). This pattern of degradation products is not observed in the pcDNA3-only lane in Fig. 8A due to the shorter exposure time used. This suggested that stabilities were similar between endogenously and exogenously transfected MEF2D (wild type and mutated). However, when PKA was coexpressed with MEF2D, we were surprised to observe that the MEF2D protein stability was markedly enhanced (Fig. 8A), indicating that PKA may play a role in MEF2D protein stabilization. Interestingly, one exception occurred when both PKA sites were mutated to alanine: PKA lost its stabilizing effect on the MEF2D protein level, and the normal degradation pattern was observed. We postulated that this effect was due to a structural change in MEF2D after PKA phosphorylation which renders the protein less accessible to cellular proteases. To test this possibility, limited proteolysis of PKA-treated MEF2D and untreated MEF2D was carried out. In vitro PKA-phosphorylated GST-MEF2D [full-length [aa 1 to 507] or MEF2D (87-507)] was used as a substrate for a limited proteolysis experiment which involved tryptic digestion for different time intervals (0 min, 2 min, 4 min, 15 min, 30 min, and 1 h), followed by separation and detection of degradation patterns by immunoblotting (Fig. 8C). PKA-treated MEF2D was substantively more resistant to proteolysis than untreated MEF2D, as shown in Fig. 8C. These data indicate that in addition to inhibiting MEF2D activity, PKA also stabilizes the MEF2D protein level by altering its structure, making it less accessible to cellular proteases.

To further assess the change in transactivation properties caused by full-length MEF2D mutations, the mutated and wild-type MEF2D proteins were analyzed in transcriptional gene reporter assays using a MEF2-dependent reporter gene (pGL3-4 × MEF2-Luc). First, full-length wild-type MEF2D and serine 121/190 alanine mutants were cotransfected with pGL3-4 × MEF2-Luc in C3H10T1/2 cells. Without exogenous expression of pFC-PKA, the MEF2D S121/190A mutant showed a relatively higher transactivation potential than did wild-type MEF2D and the other mutants. However, the exogenous expression of pFC-PKA repressed MEF2D activity to some extent (Fig. 8D).

Nuclear HDAC4 contributes to the PKA inhibitory effect on MEF2D. Based on the data concerning the direct targeting of MEF2D, we concluded that the PKA phosphoacceptor sites were intrinsically involved in the repression of myogenesis. However, since the alanine 121/190 mutants of full-length MEF2D were still partially repressed by PKA, we perceived that there might be an additional mechanism involved in the inhibition of MEF2 function by PKA. Given that the class II HDACs interact with and repress MEF2 activity in an analogous manner to that of PKA, we postulated that the association with class II HDACs might be involved in the PKA repression of MEF2D. In these experiments, we utilized FSK as a potent and well-characterized activator of adenylate cyclase and, subsequently, PKA (66), along with a well-characterized PKA inhibitor, *N*-[2-(*p*-bromocinnamylamino)ethyl]-5-isoquinolinesulfonamide · 2HCl (H89). Since a major level of control for the HDACs is their shuttling from the cytoplasm to the nucleus, we first tested whether this property might be modulated by PKA signaling. In C2C12 myoblasts treated with FSK, we observed a dramatic nuclear accumulation of HDAC4 compared to that in the solvent-treated control. Inhibition of PKA by H89 treatment reversed this effect, indicating that PKA activation by FSK results in the nuclear localization of HDAC4 (Fig. 9A). We also confirmed that PKA promotes the nuclear localization of HDAC4 in FSK-treated C2C12 cells by immunofluorescence analysis (Fig. 9B). Since HDAC4 is a well-documented repressor of MEF2 function, we went on to test whether PKA activation might lead to an increase in the nuclear association of HDAC4 with MEF2D. To assess this possibility, coimmunoprecipitation assays were performed in which pcDNA3-MEF2D or pcDNA3-MEF2D S121/190A and Flag-HDAC4 were transiently transfected with or without pFC-PKA. Expression of MEF2D and Flag-HDAC4 was confirmed by immunoblotting (Fig. 9C). In agreement with the observation of increased levels of HDAC4 in the nucleus with PKA activation, PKA activation also increased the stoichiometric amount of HDAC4 in complex with MEF2D (Fig. 9C).

stained with Coomassie blue. (B) Tryptic peptide mapping of PKA-treated and untreated proteins generated nearly identical mass spectra identifying them as mouse MEF2D. (C) Mass spectral windows revealing phosphopeptides previously observed in the in vitro kinase assays. (D) MEF2D 119-129 (RApSEELDGLFR) was confirmed on TAP-MEF2D with PKA overexpression. CID of the 1,372.64-Th ion generated an MS/MS spectrum almost identical to that obtained from the in vitro kinase experiment (Fig. 4A). (E) Schematic map of the two novel PKA phosphorylation sites, Ser 121 and Ser 190, in mouse MEF2D.

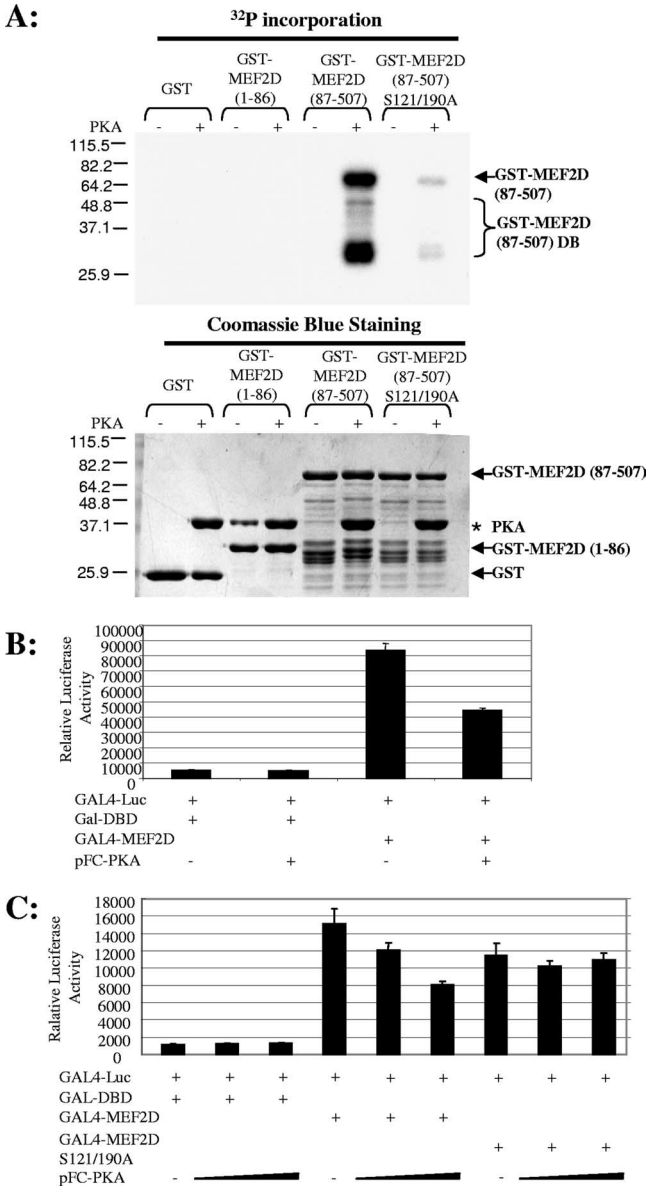

FIG. 6. PKA targets MEF2D Ser 121 and Ser 190 to inhibit transcriptional activation properties. (A) Mutation of Ser 121/190 to alanine [GST-MEF2D (87-509) S121/190A] abolishes PKA-mediated phosphorylation compared to that of wild-type MEF2D [GST-MEF2D (87-509)]. Purified GST and GST-MEF2D (aa 1 to 86 or aa 87 to 507, wild type or S121/190A mutant) were incubated in vitro, with or without purified PKA, with [γ-^{32}P]ATP, resolved using SDS-PAGE, visualized by Coomassie blue staining (lower panel), dried, and exposed to X-ray film for 30 min after the PKA kinase assay (top panel). These data are representative of two independent experiments. (B) C3H10T1/2 cells were cotransfected with GAL-DBD or GAL4-MEF2D (87-507), with or without pFC-PKA, and harvested 48 h after transfection. PKA suppressed MEF2D transcriptional activity. (C) C3H10T1/2 cells were transfected with GAL-DBD, wild-type GAL4-MEF2D (87-507), or mutated GAL4-MEF2D (87-507) S121/190A with increasing concentrations of pFC-PKA (0, 0.5, or 1 μg) and harvested 48 h after transfection. PKA suppressed wild-type GAL4-MEF2D (87-507) transcriptional activity but not that of the GAL4-MEF2D (87-507) S121/190A mutant, suggesting that the two PKA novel sites are responsible for PKA's negative regulation of MEF2D transactivation properties.

In addition, we observed no noticeable difference in the association of HDAC4 with wild-type or S121/190A mutant MEF2D, indicating that PKA phosphorylation of MEF2D does not alter the affinity of the HDAC4-MEF2D interaction. Normal mouse IgG was used in these assays as a negative control, and no protein was precipitated (data not shown). Therefore, our interpretation of these data are that a secondary effect of PKA activation is a redistribution of the HDAC4 corepressor to the nucleus, resulting in an increased stoichiometry of the HDAC4-MEF2D interaction. To address whether the increased HDAC4-MEF2D association plays a role in PKA-mediated inhibition, we performed transcriptional gene reporter assays using trichostatin (TSA), which inhibits HDAC activity. We document that under conditions of HDAC inhibition, we still observed a robust inhibition of MEF2D activity by PKA, indicating that a considerable fraction of the PKA repression of MEF2D does not rely on HDAC4 activity (Fig. 10A). However, we did observe a more pronounced PKA inhibition of MEF2D without TSA treatment, indicating that HDAC recruitment is a component of the inhibition. Also, TSA treatment fully rescued the diminished PKA-mediated repression of S121/190A mutant MEF2D, whereas only partial rescue of activity of wild-type MEF2D was observed. These data support both direct and indirect mechanisms in the functional repression of MEF2D by PKA, although the pronounced inhibition of wild-type MEF2D activity by PKA when HDAC activity is blocked suggests that the direct phosphorylation of MEF2D by PKA is the primary mechanism of inhibition. This is supported in our other studies suggesting that the structure of MEF2D is altered in response to PKA phosphorylation.

To address whether PKA might regulate MEF2D DNA binding properties, EMSAs were performed. In these experiments, we observed that the MEF2D S121/190A mutant still retained the ability to bind to DNA in a manner similar to that of wild-type MEF2D (Fig. 10B). In addition, PKA did not alter the DNA binding activity of either wild-type or S121/190A mutant MEF2D. Interestingly, when HDAC4 was cotransfected with PKA and MEF2D, we observed a stabilization of MEF2D binding to DNA that was consistent for both wild-type and S121/190A mutant MEF2D.

cAMP activation abrogates MEF2 activity in the MEF2-LacZ sensor mouse. In order to begin to determine the role of cAMP-dependent PKA signaling in MEF2 activity in vivo, we used the MEF2 sensor mouse (52), which contains a MEF2-driven reporter gene as an indicator of MEF2 activity (Fig. 11A). This assay has the added advantage of using a reporter gene which is embedded in a chromatin template. We made primary somite monolayer cultures from 9.5-dpc embryos, as we previously reported (17), and treated the cells with or without cell-permeative FSK to activate PKA signaling. Previous studies from our group have documented that MEF2 activity is critical for muscle differentiation in the somite myotome (17). After 24 h in culture, the cultured cells were stained with X-Gal to observe MEF2 activity. Compared with the results under control conditions, the number of MEF2 β-Gal-positive cells was reduced about 40% and 70% in the FSK (10 μM and 30 μM)-treated somite cultures, respectively (Fig. 11A). In addition, we carried out an in vivo PKA activation treatment with the MEF2-LacZ sensor mouse by injecting the gastrocnemii

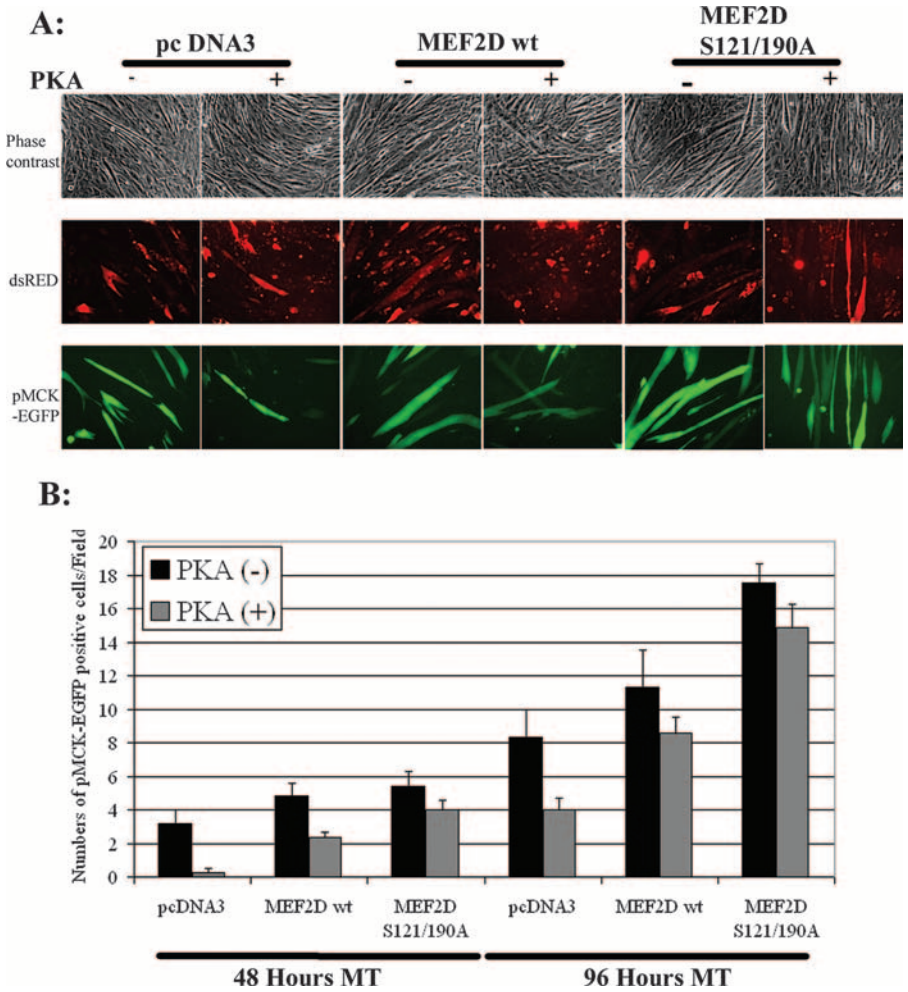

FIG. 7. PKA-resistant MEF2D S121/190A mutation enhances myogenesis and counteracts PKA-mediated myogenic repression. (A) C2C12 myoblasts were transiently transfected with either empty vector (pcDNA3) or pcDNA3-MEF2D (wild type or alanine mutant), with or without pFC-PKA. pMCK-EGFP and pCMV-dsRed2 were transfected under each condition. Cells were allowed to recover in GM for 24 h and to differentiate in DM for 96 h. Phase-contrast and fluorescence images (green, pMCK-EGFP; and red, pCMV-dsRed2) were obtained at 96 h. Cells expressing MEF2D S121/190A were resistant to PKA inhibition, exhibiting differentiation equivalent to that of the control. (B) The number of GFP-positive cells at 48 h and 96 h was counted under each condition. Values are the means ± SEM calculated from more than eight fields of view in three separate experiments. MT, myotubes.

of postnatal mice with FSK (100 μM) or a saline control, and we subsequently documented MEF2-LacZ activity at 24 h postinjection. In parallel with our results for embryonic somite cultures, we observed that MEF2 activity was markedly reduced in the FSK-treated gastrocnemii compared to that in the controls (Fig. 11B). In addition, compared to the controls, a substantive reduction of MEF2 activity was also observed in the gastrocnemius muscle when the phosphodiesterase inhibitor IBMX (1.5 mM) was used to increase intracellular cAMP levels (Fig. 11B). Also, previous experiments from our lab have shown that a direct intramuscular injection of barium chloride ($BaCl_2$) causes a marked degeneration of the muscle followed by a robust regeneration which involves MEF2 activation (1). Using this model system, we asked the question of whether PKA activation by IBMX would abrogate the regeneration-associated activation of MEF2. Indeed, we observed a pronounced reduction of MEF2 activation when the regenerating muscle was treated with IBMX (Fig. 11C). In support of the observations using FSK, IBMX treatment also caused a diminution of MEF2 activity in control muscle. Collectively, these data indicate that activation of PKA signaling can repress MEF2 function in embryonic and postnatal skeletal muscle.

DISCUSSION

PKA signaling potently represses skeletal muscle differentiation, although the exact molecular mechanism has not yet been defined precisely. In this report, we document a novel convergence of PKA signaling on the MEF2D transcriptional regulator during skeletal myogenesis. These studies characterize a potent inhibitory effect of PKA on the transactivation properties of MEF2D, leading to repression of the myogenic differentiation program. Detailed MS-based characterization of the PKA phosphoacceptor sites on MEF2D identified Ser 121 and Ser 190 as the PKA-phosphorylated residues. Importantly, expression of a mutated form of MEF2D in which the

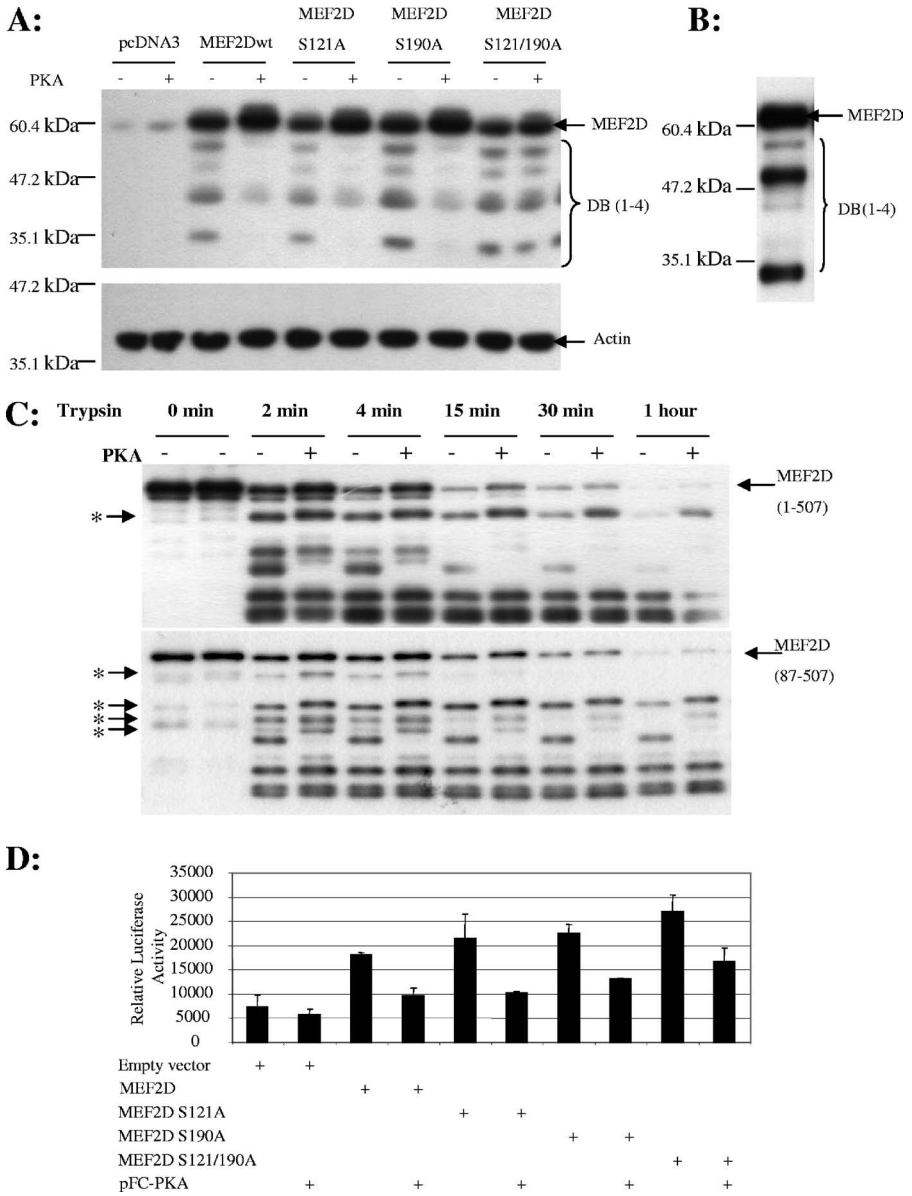

FIG. 8. PKA activation stabilizes MEF2D protein levels. (A) C3H10T1/2 cells were transfected with empty vector, full-length wild-type MEF2D, or an S121/190A single or double mutant, with or without PKA coexpression. DB, MEF2D degradation bands. Immunoblotting with anti-actin was used as a loading control to indicate that equal amounts of total protein were loaded into each lane. (B) Immunoblotting with anti-MEF2D was performed for endogenous MEF2D and identified a similar pattern of degradation bands to those seen with transfected MEF2D (shown in panel A). (C) Limited proteolysis of GST-MEF2D. Purified GST-MEF2D [5 μg full-length GST-MEF2D (1-507) or GST-MEF2D (87-507)] was incubated with or without purified PKA and with normal ATP for 30 min at 30°C. Seven equal aliquots were then taken from each sample, incubated with sequence-modified trypsin at 16°C for different time intervals, and separated by 10% SDS-PAGE. Immunoblotting by anti-MEF2D (346-511) was used to detect all nondigested and digested MEF2D peptides. These indicate that PKA-treated MEF2D is resistant to protease cleavage. (D) C3H10T1/2 cells were transfected with the pGL3-4 × MEF2-Luc reporter gene with pCMV-β-Gal and empty vector (pcDNA3) or vector for full-length wild-type MEF2D, MEF2D S121A, MEF2D S190A, or MEF2D S121/190A.

PKA phosphoacceptor sites were neutralized by conversion to alanine counteracted the inhibitory effect of PKA on myogenesis, indicating that repression of MEF2D, which is the only MEF2 isoform expressed in myoblasts prior to differentiation, is indeed a primary target of PKA-mediated myogenic repression. In addition to the direct posttranslational modification of PKA signaling on MEF2D, we further document an increase in the nuclear localization of the MEF2 corepressor HDAC4, and subsequent association with MEF2D, upon PKA activation. We posit a model in which PKA directly phosphorylates MEF2D and also promotes the association between HDAC4 and MEF2D (Fig. 12). Thus, these studies identify a key functional link between extracellular signals linked to PKA activation and the program of MEF2-dependent gene expression required for myogenic differentiation.

A pertinent question concerns what function the PKA-me-

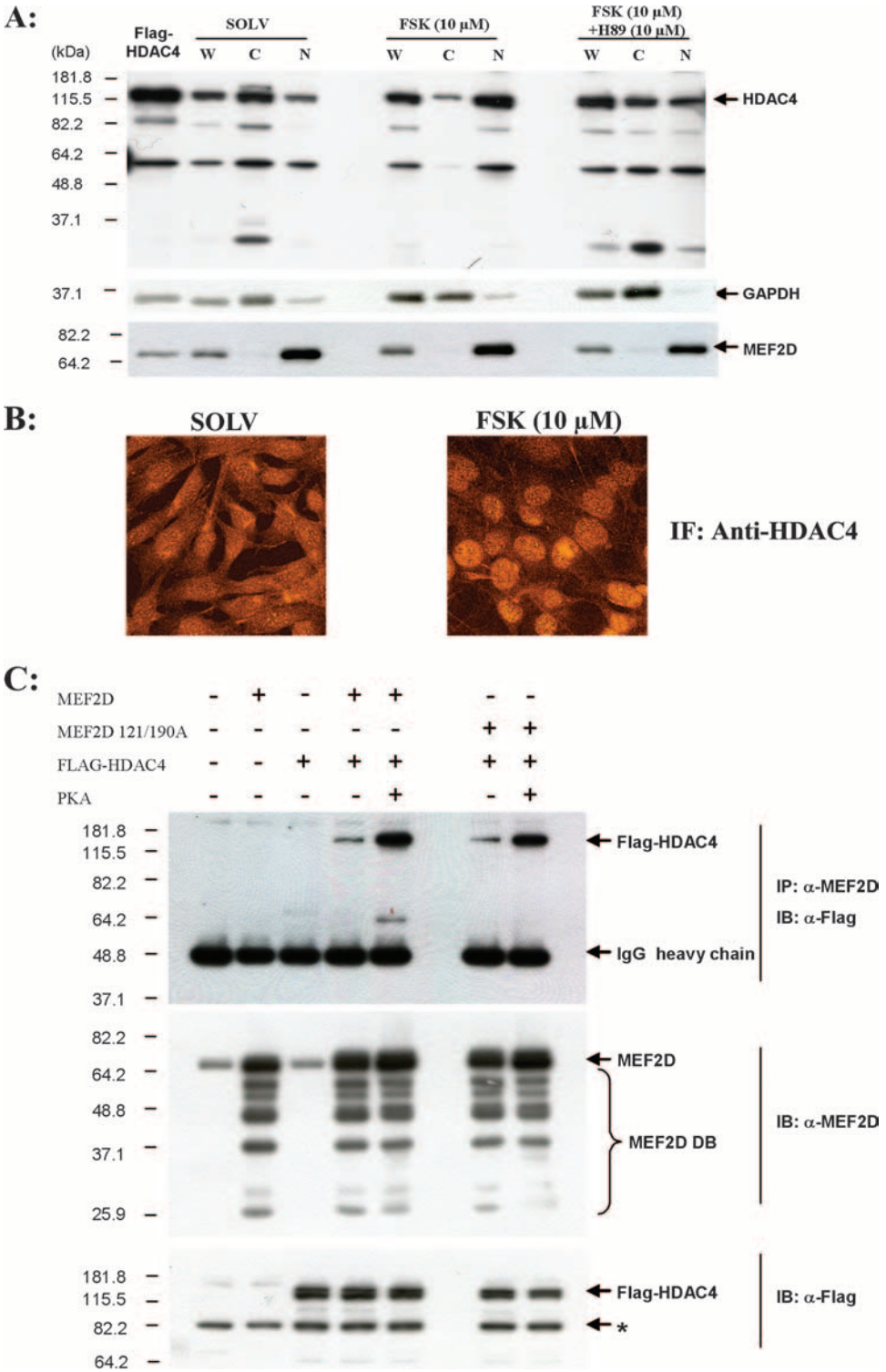

FIG. 9. PKA increases HDAC4 nuclear localization and association with MEF2D. (A) C2C12 myoblasts were cultured in low-mitogen medium for 3 h and then treated with either solvent (dimethyl sulfoxide [DMSO]), FSK (10 μM), or H89 (PKA inhibitor [10 μM]) for 6 h prior to being harvested. Whole-cell (W), cytoplasmic (C), and nuclear (N) extracts were obtained as described in Materials and Methods. Equal amounts of total protein (10 μg) were loaded for all samples. Western blotting was performed using anti-HDAC4 to check the HDAC4 localization. Immunoblotting using anti-glyceraldehyde-3-phosphate dehydrogenase and anti-MEF2D was used as cytoplasmic and nuclear fraction markers, respectively. (B) C2C12 myoblasts were cultured in low-mitogen medium for 3 h and then treated with either solvent (DMSO) or FSK (10 μM) for 6 h prior to 4% formaldehyde fixation. Indirect immunocytochemistry was performed by using anti-HDAC4. The images were captured using a Fluoview 300 (Olympus) confocal microscope. (C) Cos7 cells were transfected with the indicated combinations of pcDNA3, Flag-HDAC4, pcDNA3-MEF2D, pcDNA3-MEF2D S121/190A, and pFC-PKA. Coimmunoprecipitation was performed using anti-MEF2D and immunoblotted with anti-MEF2D or anti-Flag (for HDAC4 detection). (Top) PKA treatment resulted in qualitatively more Flag-HDAC4 association with MEF2D and MEF2D S121/190A. (Middle and bottom) Immunoblots of cell lysates showing the expression of MEF2D and Flag-HDAC4 used in the coimmunoprecipitation experiment.

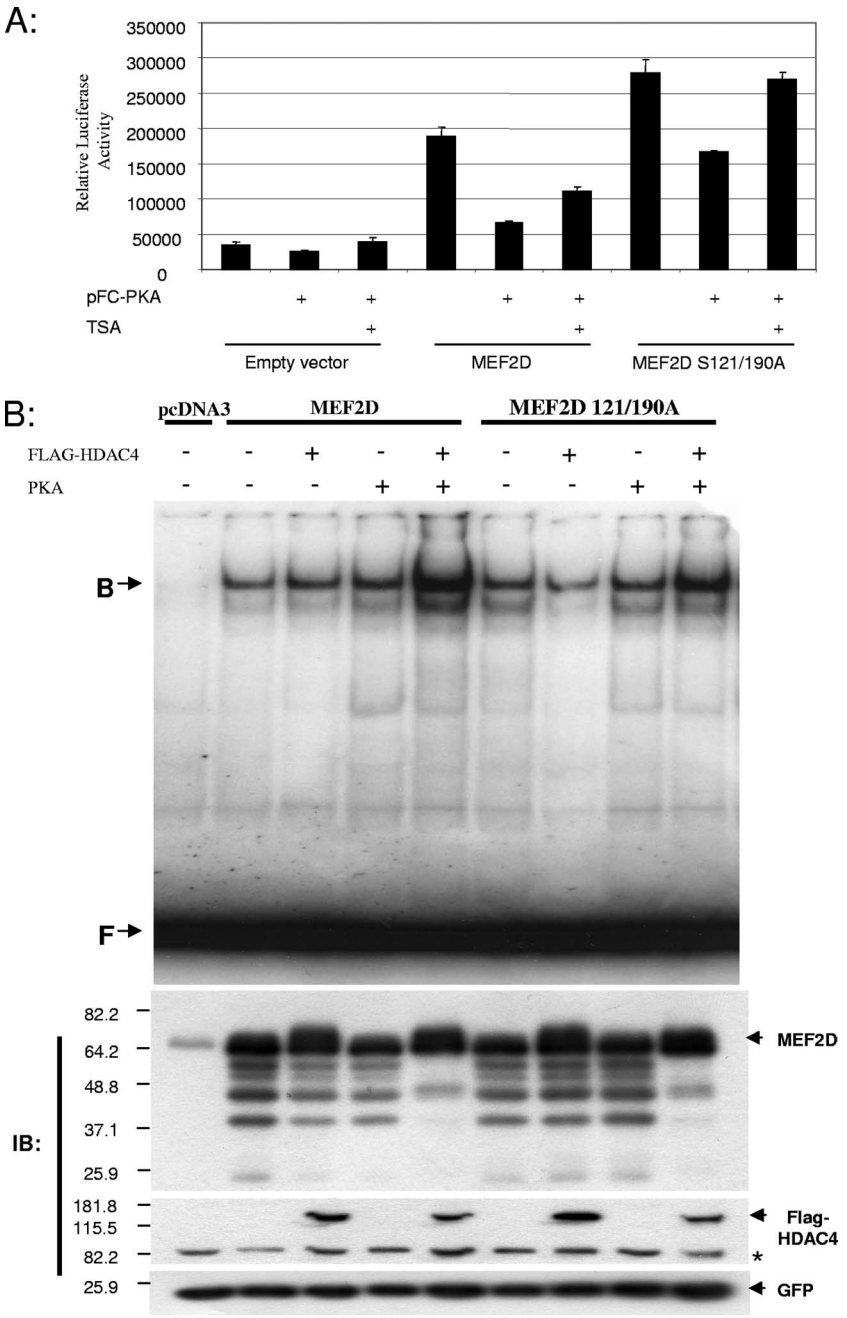

FIG. 10. HDAC activity contributes to the PKA inhibitory effect on MEF2D. (A) Cos7 cells were transfected with empty vector or pcDNA3-MEF2D (wild type or mutant [S121/190A]), with and without pFC-PKA. pGL3-4 × MEF2-Luc was used as the reporter gene. pCMV-β-galactosidase was transfected as an internal control for transfection efficiency. Cells were treated with or without 0.1 μM TSA for 16 h prior to being harvested. (B) EMSA was used to determine whether PKA modulates MEF2D DNA binding properties. (Top) PKA does not alter the DNA binding properties of wild-type MEF2D or S121/190A mutant MEF2D. The inclusion of HDAC4 with PKA does appear to stabilize the MEF2D DNA binding complex. (Bottom) Western blots of the extracts used in EMSA.

diated repression of MEF2 activity might fulfill in vivo. Previously, it was documented that PKA regulates somite myogenesis in the early phase of myogenic induction by targeting CREB (11). Analysis of the pattern of PKA-mediated CREB Ser 133 phosphorylation revealed that it is dynamically regulated in the early phase of myogenic commitment in the somite at the time when Pax3 is expressed and just as Myf5 and MyoD are being expressed in the medial and lateral dermomyotomal ridges, at around 9.5 dpc in the mouse (11). As the myotome forms and cells begin to differentiate, Ser133-phosphorylated CREB is downregulated, indicating that PKA signaling in the myotome is subsequently attenuated once the cells are committed to the myogenic lineage. Interestingly, we previously documented that MEF2A and -D are expressed in the somite

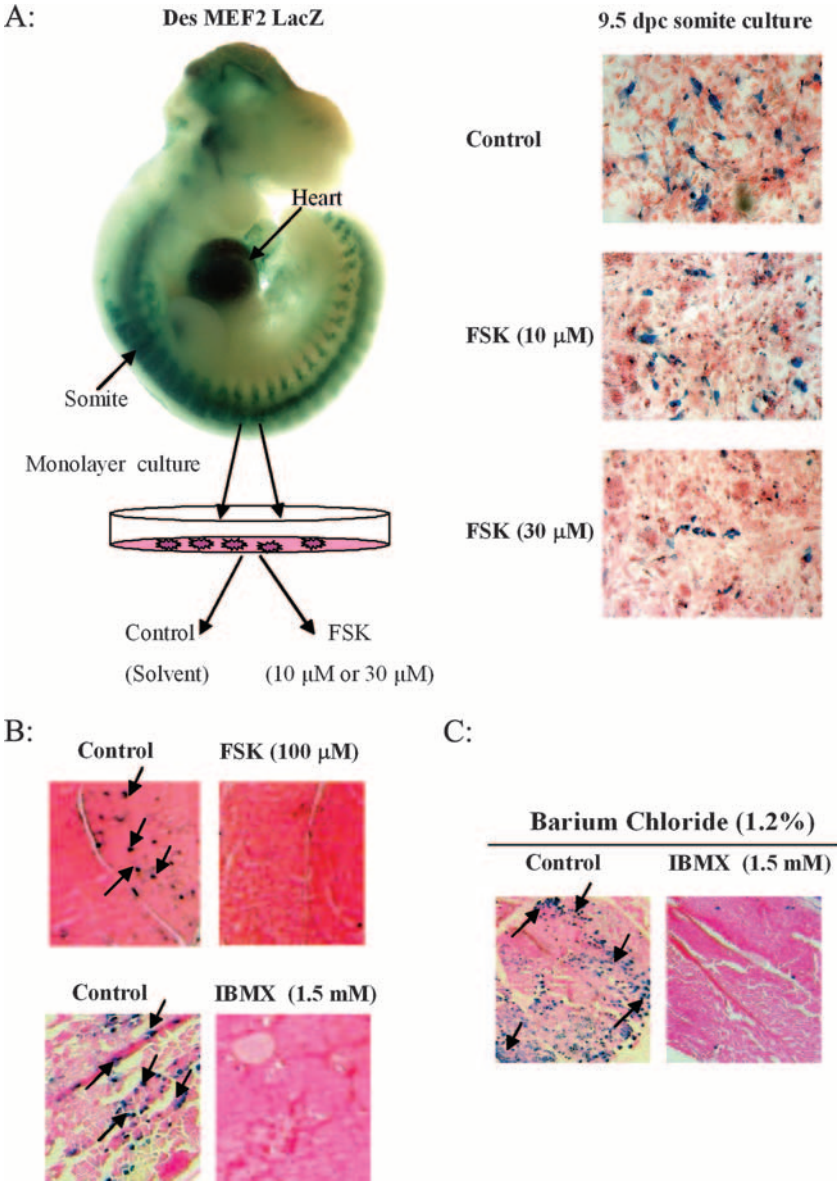

FIG. 11. cAMP activation abrogates MEF2 activity in the MEF2 sensor mouse. (A) The whole embryo picture of a MEF2 sensor mouse at 9.5 dpc indicates the expression of the MEF2-LacZ transgene as previously described (52). Dissected interlimb somites were cultured in a monolayer, as we previously described (17), with normal GM and solvent (DMSO) or FSK (10 μM or 30 μM) and then stained with X-Gal. (B) The gastrocnemius muscles of the left hindlimbs were injected with 100 μl FSK in PBS at a concentration of 100 μM or with the phosphodiesterase inhibitor IBMX at a concentration of 1.5 mM. The gastrocnemius muscles of the right hindlimbs served as controls. Twenty-four hours after FSK injection, transverse sections of leg muscles were made and stained for β-galactosidase. Representative images of the lateral region of the gastrocnemius at the injection site are shown. (C) The gastrocnemius muscles of both hindlimbs were injected with barium chloride (1.2%) to induce degeneration and regeneration. The gastrocnemius muscle of one hindlimb served as a control, and the other hindlimb was injected with IBMX (1.5 mM). Twenty-four hours after injection, transverse sections of leg muscles were prepared and stained for β-Gal. Representative images of the lateral regions of the gastrocnemii at the injection site are shown.

beginning at 8.5 to 9 dpc (19). Our previous data showed that MEF2 activation, as indicated in a transgenic mouse carrying a LacZ reporter gene driven by MEF2 binding sites, occurs at around 9.5 dpc and is required for myotomal myogenesis, since attenuation of MEF2 activity by inhibiting p38 MAPK signaling blocks myotomal differentiation but not commitment to the myogenic lineage (17). Moreover, in the present study we document that activation of PKA results in repression of MEF2 activity in primary somite cultures from 9.5-dpc mouse embryos. Based on these observations, we postulate that one role of PKA signaling in the early somite, apart from positively targeting CREB activity, is to repress MEF2 transactivation properties, a function required to prevent precocious differentiation of the cells committed to the myogenic lineage. Interestingly, a recent report documented that CREB-mediated activation of a kinase named SIK1 can lead to phosphorylation and export of class II HDACs from the nuclei in muscle cells. Importantly, this study showed that cAMP signaling can inac-

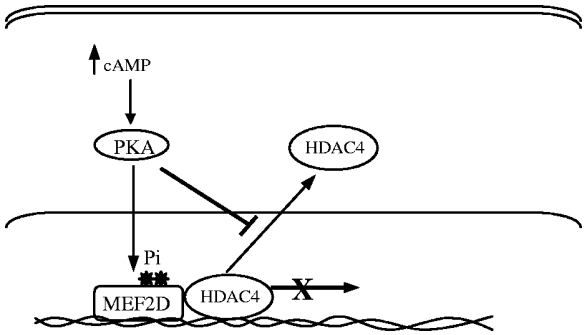

FIG. 12. Schematic model of the bipartite mechanism of MEF2D targeting by PKA during myogenesis, showing (i) direct phosphorylation of MEF2D at Ser 121 and Ser 190 and (ii) enhancement of HDAC4 nuclear accumulation and physical association with MEF2D.

tivate SIK1 and increase the nuclear accumulation of HDAC5 (6). Thus, a reciprocal connection between CREB and MEF2 may be coordinated by PKA signaling. This proposed dual function of PKA signaling is consistent with the idea that CREB activation is required for Wnt-mediated expression of the early myogenic commitment markers, Pax3, MyoD, and Myf5, at a time when the cells maintain their proliferative potential (11). Once the cell population committed to the myogenic fate is established by the expression of commitment markers and the cell numbers are sufficiently expanded, PKA signaling is downregulated, allowing MEF2 to activate its target genes and contribute to the program of myotomal differentiation.

Another possible role of PKA in MEF2 signaling is indicated by studies assessing the role of cAMP signaling in the central nervous system. Previous studies have implicated MEF2 as a calcium-dependent prosurvival factor to protect neurons from apoptosis (37, 42, 43, 53). A recent report has indicated that increasing intracellular cAMP levels inhibit Ca^{2+}-mediated activation of MEF2D (5). Our studies are in agreement with this study and further show that cAMP signaling modulates MEF2 function via activation of PKA. These observations may provide important insight into the regulation of MEF2 activity in neuronal cell survival pathways. Interestingly, MEF2 also plays a pivotal role in transcriptional regulation in several other cell types, such as cardiomyocytes and smooth muscle cells, that are also highly responsive to adrenergic hormones that activate the adenylate cyclase-cAMP-PKA signaling pathway. Thus, it will be of significant interest to determine the conservation and function of this PKA-MEF2 signaling conduit for the regulation of MEF2-dependent gene expression in these other cell types.

Recently, it was reported that an intersection between cAMP signaling and MAPK cascades occurs under conditions in which elevated levels of cAMP-induced PKA activation result in abrogation of ERK5 but not ERK1/2 signaling (60). Interestingly, our group and others have shown that ERK5, but not ERK1/2, directly targets and activates MEF2 transactivation properties (31, 76). Whether the downregulation of MEF2 activity in response to PKA activation is partially dependent on abrogation of ERK5 signaling is a remaining question, although our data indicate that PKA can directly target MEF2 phosphorylation and activity in the absence of ERK5 activity, at least in some cellular contexts. However, since PKA activation negatively regulates MEF2 activity and, conversely, ERK5 and p38 MAPK positively upregulate activity, it is nevertheless pertinent to consider the issue of functional dominance when multiple kinase signals converge on one target protein, in this case MEF2. Importantly, the outcome of multiple kinase signal cascades on gene expression will ultimately be determined by the interpretation of the combination of signals converging on a transcriptional regulator at any moment. In this regard, MEF2 regulation by positive (ERK5/p38 MAPK) and negative (PKA) signaling may prove a useful model system to determine how convergence of multiplex signaling events on one transcription factor can produce unique combinatorial or hierarchical responses in target gene activation.

In summary, these studies document a novel repressive role for PKA signaling to the MEF2D transcription factor during skeletal myogenesis. The function of PKA signaling to MEF2D may have important implications for skeletal muscle differentiation during mammalian embryogenesis and also for the response to cAMP signaling in a variety of postnatal MEF2-dependent cell types.

ACKNOWLEDGMENTS

We thank Xu Guo from Applied Biosystems/MDS Sciex for assistance in performing nano-LC-MS/MS. We thank Tetsuaki Miyake for technical assistance. We also thank Lee Wong in the York University Core Molecular Biology Facility for DNA sequencing.

These studies were made possible by a grant from the Canadian Institute of Health Research (CIHR) to J.C.M. Salary support for R.L.S.P. was provided in part by a postdoctoral fellowship from the Muscular Dystrophy Association of Canada (MDAC) and CIHR. Infrastructural support was provided by the Ontario Research and Development Challenge Fund and Applied Biosystems/MDS SCIEX to K.W.M.S. Seneca College Office of Research and Innovation is acknowledged for providing release time support for J. W. Gordon.

REFERENCES

1. **Akkila, W. M., R. L. Chambers, O. I. Ornatsky, and J. C. McDermott.** 1997. Molecular cloning of up-regulated cytoskeletal genes from regenerating skeletal muscle: potential role of myocyte enhancer factor 2 proteins in the activation of muscle-regeneration-associated genes. Biochem. J. **325:**87–93.
2. **Amacher, S. L., J. N. Buskin, and S. D. Hauschka.** 1993. Multiple regulatory elements contribute differentially to muscle creatine kinase enhancer activity in skeletal and cardiac muscle. Mol. Cell. Biol. **13:**2753–2764.
3. **Anderson, J. P., E. Dodou, A. B. Heidt, S. J. De Val, E. J. Jaehnig, S. B. Greene, E. N. Olson, and B. L. Black.** 2004. HRC is a direct transcriptional target of MEF2 during cardiac, skeletal, and arterial smooth muscle development in vivo. Mol. Cell. Biol. **24:**3757–3768.
4. **Arnold, H. H., and B. Winter.** 1998. Muscle differentiation: more complexity to the network of myogenic regulators. Curr. Opin. Genet. Dev. **8:**539–544.
5. **Belfield, J. L., C. Whittaker, M. Z. Cader, and S. Chawla.** 2006. Differential effects of Ca2+ and cAMP on transcription mediated by MEF2D and cAMP-response element-binding protein in hippocampal neurons. J. Biol. Chem. **281:**27724–27732.
6. **Berdeaux, R., N. Goebel, L. Banaszynski, H. Takemori, T. Wandless, G. D. Shelton, and M. Montminy.** 2007. SIK1 is a class II HDAC kinase that promotes survival of skeletal myocytes. Nat. Med. **13:**597–603.
7. **Black, B. L., and E. N. Olson.** 1998. Transcriptional control of muscle development by myocyte enhancer factor-2 (MEF2) proteins. Annu. Rev. Cell Dev. Biol. **14:**167–196.
8. **Brand-Saberi, B.** 2005. Genetic and epigenetic control of skeletal muscle development. Ann. Anat. **187:**199–207.
9. **Buckingham, M.** 2006. Myogenic progenitor cells and skeletal myogenesis in vertebrates. Curr. Opin. Genet. Dev. **16:**525–532.
10. **Buckingham, M.** 2001. Skeletal muscle formation in vertebrates. Curr. Opin. Genet. Dev. **11:**440–448.
11. **Chen, A. E., D. D. Ginty, and C. M. Fan.** 2005. Protein kinase A signalling via CREB controls myogenesis induced by Wnt proteins. Nature **433:**317–322.
12. **Cox, D. M., M. Du, X. Guo, K. W. Siu, and J. C. McDermott.** 2002. Tandem affinity purification of protein complexes from mammalian cells. BioTechniques **33:**267–270.

13. **Cox, D. M., M. Du, M. Marback, E. C. Yang, J. Chan, K. W. Siu, and J. C. McDermott.** 2003. Phosphorylation motifs regulating the stability and function of myocyte enhancer factor 2A. J. Biol. Chem. **278:**15297–15303.
14. **Creemers, E. E., L. B. Sutherland, J. McAnally, J. A. Richardson, and E. N. Olson.** 2006. Myocardin is a direct transcriptional target of Mef2, Tead and Foxo proteins during cardiovascular development. Development **133:**4245–4256.
15. **Creemers, E. E., L. B. Sutherland, J. Oh, A. C. Barbosa, and E. N. Olson.** 2006. Coactivation of MEF2 by the SAP domain proteins myocardin and MASTR. Mol. Cell **23:**83–96.
16. **Currie, P. D., and P. W. Ingham.** 1998. The generation and interpretation of positional information within the vertebrate myotome. Mech. Dev. **73:**3–21.
17. **de Angelis, L., J. Zhao, J. J. Andreucci, E. N. Olson, G. Cossu, and J. C. McDermott.** 2005. Regulation of vertebrate myotome development by the p38 MAP kinase-MEF2 signaling pathway. Dev. Biol. **283:**171–179.
18. **Donoviel, D. B., M. A. Shield, J. N. Buskin, H. S. Haugen, C. H. Clegg, and S. D. Hauschka.** 1996. Analysis of muscle creatine kinase gene regulatory elements in skeletal and cardiac muscles of transgenic mice. Mol. Cell. Biol. **16:**1649–1658.
19. **Edmondson, D. G., G. E. Lyons, J. F. Martin, and E. N. Olson.** 1994. Mef2 gene expression marks the cardiac and skeletal muscle lineages during mouse embryogenesis. Development **120:**1251–1263.
20. **Ewton, D. Z., and J. R. Florini.** 1990. Effects of insulin-like growth factors and transforming growth factor-beta on the growth and differentiation of muscle cells in culture. Proc. Soc. Exp. Biol. Med. **194:**76–80.
21. **Florini, J. R., D. Z. Ewton, and K. A. Magri.** 1991. Hormones, growth factors, and myogenic differentiation. Annu. Rev. Physiol. **53:**201–216.
22. **Florini, J. R., D. Z. Ewton, K. A. Magri, and F. J. Mangiacapra.** 1993. IGFs and muscle differentiation. Adv. Exp. Med. Biol. **343:**319–326.
23. **Gong, X., X. Tang, M. Wiedmann, X. Wang, J. Peng, D. Zheng, L. A. Blair, J. Marshall, and Z. Mao.** 2003. Cdk5-mediated inhibition of the protective effects of transcription factor MEF2 in neurotoxicity-induced apoptosis. Neuron **38:**33–46.
24. **Grayson, J., R. Bassel-Duby, and R. S. Williams.** 1998. Collaborative interactions between MEF-2 and Sp1 in muscle-specific gene regulation. J. Cell. Biochem. **70:**366–375.
25. **Gregoire, S., and X. J. Yang.** 2005. Association with class IIa histone deacetylases upregulates the sumoylation of MEF2 transcription factors. Mol. Cell. Biol. **25:**2273–2287.
26. **Han, J., Y. Jiang, Z. Li, V. V. Kravchenko, and R. J. Ulevitch.** 1997. Activation of the transcription factor MEF2C by the MAP kinase p38 in inflammation. Nature **386:**296–299.
27. **Hanson, M. G., Jr., S. Shen, A. P. Wiemelt, F. A. McMorris, and B. A. Barres.** 1998. Cyclic AMP elevation is sufficient to promote the survival of spinal motor neurons in vitro. J. Neurosci. **18:**7361–7371.
28. **Horikawa, M., S. Higashiyama, S. Nomura, Y. Kitamura, M. Ishikawa, and N. Taniguchi.** 1999. Upregulation of endogenous heparin-binding EGF-like growth factor and its role as a survival factor in skeletal myotubes. FEBS Lett. **459:**100–104.
29. **Husmann, I., L. Soulet, J. Gautron, I. Martelly, and D. Barritault.** 1996. Growth factors in skeletal muscle regeneration. Cytokine Growth Factor Rev. **7:**249–258.
30. **Jordan, M., A. Schallhorn, and F. M. Wurm.** 1996. Transfecting mammalian cells: optimization of critical parameters affecting calcium-phosphate precipitate formation. Nucleic Acids Res. **24:**596–601.
31. **Kato, Y., V. V. Kravchenko, R. I. Tapping, J. Han, R. J. Ulevitch, and J. D. Lee.** 1997. BMK1/ERK5 regulates serum-induced early gene expression through transcription factor MEF2C. EMBO J. **16:**7054–7066.
32. **Lemercier, C., A. Verdel, B. Galloo, S. Curtet, M. P. Brocard, and S. Khochbin.** 2000. mHDA1/HDAC5 histone deacetylase interacts with and represses MEF2A transcriptional activity. J. Biol. Chem. **275:**15594–15599.
33. **Li, L., R. Heller-Harrison, M. Czech, and E. N. Olson.** 1992. Cyclic AMP-dependent protein kinase inhibits the activity of myogenic helix-loop-helix proteins. Mol. Cell. Biol. **12:**4478–4485.
34. **Li, M., X. Wang, M. K. Meintzer, T. Laessig, M. J. Birnbaum, and K. A. Heidenreich.** 2000. Cyclic AMP promotes neuronal survival by phosphorylation of glycogen synthase kinase 3beta. Mol. Cell. Biol. **20:**9356–9363.
35. **Lin, Q., J. Lu, H. Yanagisawa, R. Webb, G. E. Lyons, J. A. Richardson, and E. N. Olson.** 1998. Requirement of the MADS-box transcription factor MEF2C for vascular development. Development **125:**4565–4574.
36. **Lin, Q., J. Schwarz, C. Bucana, and E. N. Olson.** 1997. Control of mouse cardiac morphogenesis and myogenesis by transcription factor MEF2C. Science **276:**1404–1407.
37. **Linseman, D. A., C. M. Bartley, S. S. Le, T. A. Laessig, R. J. Bouchard, M. K. Meintzer, M. Li, and K. A. Heidenreich.** 2003. Inactivation of the myocyte enhancer factor-2 repressor histone deacetylase-5 by endogenous Ca(2+)/calmodulin-dependent kinase II promotes depolarization-mediated cerebellar granule neuron survival. J. Biol. Chem. **278:**41472–41481.
38. **Lu, J., T. A. McKinsey, C. L. Zhang, and E. N. Olson.** 2000. Regulation of skeletal myogenesis by association of the MEF2 transcription factor with class II histone deacetylases. Mol. Cell **6:**233–244.
39. **Ludolph, D. C., and S. F. Konieczny.** 1995. Transcription factor families: muscling in on the myogenic program. FASEB J. **9:**1595–1604.
40. **Ma, K., J. K. Chan, G. Zhu, and Z. Wu.** 2005. Myocyte enhancer factor 2 acetylation by p300 enhances its DNA binding activity, transcriptional activity, and myogenic differentiation. Mol. Cell. Biol. **25:**3575–3582.
41. **Makarevich, A., A. Sirotkin, P. Chrenek, J. Bulla, and L. Hetenyi.** 2000. The role of IGF-I, cAMP/protein kinase A and MAP-kinase in the control of steroid secretion, cyclic nucleotide production, granulosa cell proliferation and preimplantation embryo development in rabbits. J. Steroid Biochem. Mol. Biol. **73:**123–133.
42. **Mao, Z., A. Bonni, F. Xia, M. Nadal-Vicens, and M. E. Greenberg.** 1999. Neuronal activity-dependent cell survival mediated by transcription factor MEF2. Science **286:**785–790.
43. **Mao, Z., and M. Wiedmann.** 1999. Calcineurin enhances MEF2 DNA binding activity in calcium-dependent survival of cerebellar granule neurons. J. Biol. Chem. **274:**31102–31107.
44. **Martin, J. F., J. M. Miano, C. M. Hustad, N. G. Copeland, N. A. Jenkins, and E. N. Olson.** 1994. A Mef2 gene that generates a muscle-specific isoform via alternative mRNA splicing. Mol. Cell. Biol. **14:**1647–1656.
45. **Miska, E. A., C. Karlsson, E. Langley, S. J. Nielsen, J. Pines, and T. Kouzarides.** 1999. HDAC4 deacetylase associates with and represses the MEF2 transcription factor. EMBO J. **18:**5099–5107.
46. **Molkentin, J. D., B. L. Black, J. F. Martin, and E. N. Olson.** 1995. Cooperative activation of muscle gene expression by MEF2 and myogenic bHLH proteins. Cell **83:**1125–1136.
47. **Molkentin, J. D., B. L. Black, J. F. Martin, and E. N. Olson.** 1996. Mutational analysis of the DNA binding, dimerization, and transcriptional activation domains of MEF2C. Mol. Cell. Biol. **16:**2627–2636.
48. **Molkentin, J. D., L. Li, and E. N. Olson.** 1996. Phosphorylation of the MADS-box transcription factor MEF2C enhances its DNA binding activity. J. Biol. Chem. **271:**17199–17204.
49. **Molkentin, J. D., and E. N. Olson.** 1996. Combinatorial control of muscle development by basic helix-loop-helix and MADS-box transcription factors. Proc. Natl. Acad. Sci. USA **93:**9366–9373.
50. **Morin, S., F. Charron, L. Robitaille, and M. Nemer.** 2000. GATA-dependent recruitment of MEF2 proteins to target promoters. EMBO J. **19:**2046–2055.
51. **Naya, F. J., and E. Olson.** 1999. MEF2: a transcriptional target for signaling pathways controlling skeletal muscle growth and differentiation. Curr. Opin. Cell Biol. **11:**683–688.
52. **Naya, F. J., C. Wu, J. A. Richardson, P. Overbeek, and E. N. Olson.** 1999. Transcriptional activity of MEF2 during mouse embryogenesis monitored with a MEF2-dependent transgene. Development **126:**2045–2052.
53. **Okamoto, S., D. Krainc, K. Sherman, and S. A. Lipton.** 2000. Antiapoptotic role of the p38 mitogen-activated protein kinase-myocyte enhancer factor 2 transcription factor pathway during neuronal differentiation. Proc. Natl. Acad. Sci. USA **97:**7561–7566.
54. **Olson, E. N.** 1990. MyoD family: a paradigm for development? Genes Dev. **4:**1454–1461.
55. **Ornatsky, O. I., J. J. Andreucci, and J. C. McDermott.** 1997. A dominant-negative form of transcription factor MEF2 inhibits myogenesis. J. Biol. Chem. **272:**33271–33278.
56. **Ornatsky, O. I., D. M. Cox, P. Tangirala, J. J. Andreucci, Z. A. Quinn, J. L. Wrana, R. Prywes, Y. T. Yu, and J. C. McDermott.** 1999. Post-translational control of the MEF2A transcriptional regulatory protein. Nucleic Acids Res. **27:**2646–2654.
57. **Ornatsky, O. I., and J. C. McDermott.** 1996. MEF2 protein expression, DNA binding specificity and complex composition, and transcriptional activity in muscle and non-muscle cells. J. Biol. Chem. **271:**24927–24933.
58. **Ottens, A. K., F. H. Kobeissy, R. A. Wolper, W. E. Haskins, R. L. Hayes, N. D. Denslow, and K. K. Wang.** 2005. A multidimensional differential proteomic platform using dual-phase ion-exchange chromatography–polyacrylamide gel electrophoresis/reversed-phase liquid chromatography tandem mass spectrometry. Anal. Chem. **77:**4836–4845.
59. **Park, S. Y., H. M. Shin, and T. H. Han.** 2002. Synergistic interaction of MEF2D and Sp1 in activation of the CD14 promoter. Mol. Immunol. **39:**25–30.
60. **Pearson, G. W., S. Earnest, and M. H. Cobb.** 2006. Cyclic AMP selectively uncouples mitogen-activated protein kinase cascades from activating signals. Mol. Cell. Biol. **26:**3039–3047.
61. **Pirskanen, A., J. C. Kiefer, and S. D. Hauschka.** 2000. IGFs, insulin, Shh, bFGF, and TGF-beta1 interact synergistically to promote somite myogenesis in vitro. Dev. Biol. **224:**189–203.
62. **Pownall, M. E., M. K. Gustafsson, and C. P. Emerson, Jr.** 2002. Myogenic regulatory factors and the specification of muscle progenitors in vertebrate embryos. Annu. Rev. Cell Dev. Biol. **18:**747–783.
63. **Quinn, Z. A., C. C. Yang, J. L. Wrana, and J. C. McDermott.** 2001. Smad proteins function as co-modulators for MEF2 transcriptional regulatory proteins. Nucleic Acids Res. **29:**732–742.
64. **Rydel, R. E., and L. A. Greene.** 1988. cAMP analogs promote survival and neurite outgrowth in cultures of rat sympathetic and sensory neurons independently of nerve growth factor. Proc. Natl. Acad. Sci. USA **85:**1257–1261.
65. **Sartorelli, V., J. Huang, Y. Hamamori, and L. Kedes.** 1997. Molecular

mechanisms of myogenic coactivation by p300: direct interaction with the activation domain of MyoD and with the MADS box of MEF2C. Mol. Cell. Biol. **17:**1010–1026.

66. **Seamon, K. B., and J. W. Daly.** 1981. Forskolin: a unique diterpene activator of cyclic AMP-generating systems. J. Cyclic Nucleotide Res. **7:**201–224.
67. **Shore, P., and A. D. Sharrocks.** 1995. The MADS-box family of transcription factors. Eur. J. Biochem. **229:**1–13.
68. **Sirotkin, A. V., and R. Grossmann.** 2006. The role of protein kinase A and cyclin-dependent (CDC2) kinase in the control of basal and IGF-II-induced proliferation and secretory activity of chicken ovarian cells. Anim. Reprod. Sci. **92:**169–181.
69. **Sirotkin, A. V., P. Sanislo, H. J. Schaeffer, I. Florkovicova, J. Kotwica, J. Bulla, and L. Hetenyi.** 2004. Thrombopoietin regulates proliferation, apoptosis, secretory activity and intracellular messengers in porcine ovarian follicular cells: involvement of protein kinase A. J. Endocrinol. **183:**595–604.
70. **Tajbakhsh, S., and G. Cossu.** 1997. Establishing myogenic identity during somitogenesis. Curr. Opin. Genet. Dev. **7:**634–641.
71. **Tollefsen, S. E., R. Lajara, R. H. McCusker, D. R. Clemmons, and P. Rotwein.** 1989. Insulin-like growth factors (IGF) in muscle development. Expression of IGF-I, the IGF-I receptor, and an IGF binding protein during myoblast differentiation. J. Biol. Chem. **264:**13810–13817.
72. **Vivarelli, E., W. E. Brown, R. G. Whalen, and G. Cossu.** 1988. The expression of slow myosin during mammalian somitogenesis and limb bud differentiation. J. Cell Biol. **107:**2191–2197.
73. **Wang, X., X. Tang, M. Li, J. Marshall, and Z. Mao.** 2005. Regulation of neuroprotective activity of myocyte-enhancer factor 2 by cAMP-protein kinase A signaling pathway in neuronal survival. J. Biol. Chem. **280:**16705–16713.
74. **Winter, B., T. Braun, and H. H. Arnold.** 1993. cAMP-dependent protein kinase represses myogenic differentiation and the activity of the muscle-specific helix-loop-helix transcription factors Myf-5 and MyoD. J. Biol. Chem. **268:**9869–9878.
75. **Yamane, A., M. L. Mayo, P. Bringas, Jr., L. Chen, M. Huynh, K. Thai, L. Shum, and H. C. Slavkin.** 1997. TGF-alpha, EGF, and their cognate EGF receptor are co-expressed with desmin during embryonic, fetal, and neonatal myogenesis in mouse tongue development. Dev. Dyn. **209:**353–366.
76. **Yang, C. C., O. I. Ornatsky, J. C. McDermott, T. F. Cruz, and C. A. Prody.** 1998. Interaction of myocyte enhancer factor 2 (MEF2) with a mitogen-activated protein kinase, ERK5/BMK1. Nucleic Acids Res. **26:**4771–4777.
77. **Youn, H. D., L. Sun, R. Prywes, and J. O. Liu.** 1999. Apoptosis of T cells mediated by Ca2+-induced release of the transcription factor MEF2. Science **286:**790–793.
78. **Yun, K., and B. Wold.** 1996. Skeletal muscle determination and differentiation: story of a core regulatory network and its context. Curr. Opin. Cell Biol. **8:**877–889.